

Ship Sway, Roll, and Yaw Motions in Oblique Seas

Rodney T. Schmitke,¹ Member

A theoretical model is developed for the prediction of ship lateral motions in oblique seas. The asymptotic behavior of this model in waves that are long relative to ship beam is examined, with particular emphasis on the classical problem of rolling in beam seas. The theoretical prediction of roll damping is discussed, and the importance of including dynamic lift on appendages is emphasized. Extensive comparisons of predicted and measured roll response are made, with good agreement at all headings considered.

Introduction

ALTHOUGH considerable success has been achieved over the past two decades in the theoretical prediction of ship heave and pitch motions, the same cannot be said for the lateral plane motions of sway, roll, and yaw. Although several computer programs exist which predict lateral motions by purely theoretical means, correlation studies have shown that errors in roll prediction are generally significant, particularly for high-speed warship hull forms. This is a serious problem, because of the great impact of rolling on ship operations.

The fundamental reason for the discrepancies reported in correlation studies is inaccurate estimation of roll damping, especially at higher speeds. Development of a satisfactory theoretical procedure for estimation of roll damping has therefore been consistently identified as the single most important requirement in ship motion theory. In the absence of such a procedure, model tests are commonly performed to determine roll damping, and these data are then input into computer programs for motion prediction purposes.

Failure to make accurate estimates of roll damping may be traced to inadequate treatment of hull appendages, and in particular to the failure to include the effects of dynamic lift on such appendages as rudders and skegs. The theory presented in this paper includes these effects and consequently produces good predictions of both roll damping and roll response. This theory has basically four facets:

1. Strip theory for computing hull added-mass, wave making damping, and exciting forces.
2. Lifting surface contributions to damping and exciting forces.
3. Viscous roll damping, principally from bilge keels.
4. Hull circulatory effects.

The theoretical basis is first described, with emphasis on the lifting surface terms and viscous contributions to roll damping. Asymptotic expressions valid for waves long relative to ship beam are then derived and discussed in order to provide a physical "feel" for the mathematical model. In particular, the classical problem of lateral motions in beam seas is addressed in depth, and it is shown that as a result of the cancellation which occurs due to sway-to-roll coupling, rolling dynamics are

approximated by a single-degree-of-freedom equation similar in form to those derived by earlier researchers on an intuitive basis.

Next, roll damping is discussed, and theoretical estimates are compared with experimental measurements for several different ships, with generally good agreement. Examples are presented showing the relative significance of the various contributions to roll damping for frigate and destroyer hull forms. These show that it is essential to include dynamic lift in theoretical estimates of roll damping; without this effect, damping will be seriously underpredicted at even moderate speeds.

Finally, theoretical predictions of roll are compared with experimental data for four different ships. For three of these, the experimental measurements are obtained from full-scale trials. Agreement between predictions and measurements is generally good, and it is concluded that the theory yields results of comparable accuracy to strip-theory predictions of pitch and heave.

Equations of motion

In applying strip theory to a displacement hull, certain assumptions are standard:

1. Ship response is a linear function of wave excitation.
2. Ship length is much greater than either beam or draft.
3. All viscous effects other than roll damping are negligible.
4. The hull does not develop appreciable planing lift.

The linear equations of motion for the ship without roll stabilizers are given in the following. These are written with respect to a stability axis system fixed in the ship; this axis system is slightly different from the translating earth axes normally used in predicting ship motions in waves. Stability axes are commonly used in dynamic simulation of both aircraft and marine vehicles. In the present case, stability axes offer the advantage of being more suitable for control studies and of yielding simpler expressions for the coefficients of the equations of motion. Further, hull circulatory effects are included in the mathematical model, and expressions given in the literature for these effects are written in terms of stability axes. The axis system is illustrated in Fig. 1. The axes are fixed in the ship with origin at the CG, and in the reference condition of steady forward speed with no seaway or control disturbances, the x -axis is directed horizontally forward, the z -axis vertically upward, and the y -axis to port. The ship is assumed to be traveling at

¹ Leader, Ship Dynamics Group Defence Research Establishment Atlantic, Dartmouth, Nova Scotia, Canada.

Presented at the Annual Meeting, New York, N.Y., November 16-18, 1978, of THE SOCIETY OF NAVAL ARCHITECTS AND MARINE ENGINEERS.

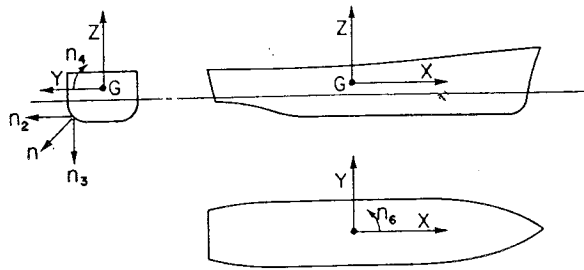


Fig. 1 Axis system

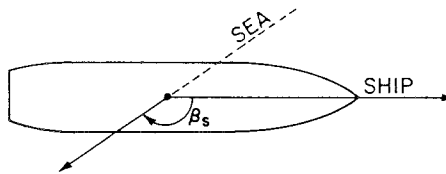


Fig. 2 Definition of sea direction

constant speed U along a mean course at angle β_s to the direction of propagation of a train of long-crested waves (Fig. 1).

The coupled sway, roll, and yaw equations follow, with notation similar to Salvesen et al [1]²:

$$\text{Sway: } (A_{22} + m)\ddot{\eta}_2 + B_{22}\dot{\eta}_2 + A_{24}\ddot{\eta}_4 + B_{24}\dot{\eta}_4 + A_{26}\ddot{\eta}_6 + (B_{26} + mU)\dot{\eta}_6 = F_2 e^{i\omega t} \quad (1)$$

$$\text{Roll: } A_{24}\ddot{\eta}_2 + B_{24}\dot{\eta}_2 + (A_{44} + I_4)\ddot{\eta}_4 + B_{44}\dot{\eta}_4 + C_{44}\eta_4 + A_{46}\ddot{\eta}_6 + B_{46}\dot{\eta}_6 = F_4 e^{i\omega t} \quad (2)$$

$$\text{Yaw: } A_{62}\ddot{\eta}_2 + B_{62}\dot{\eta}_2 + A_{64}\ddot{\eta}_4 + B_{64}\dot{\eta}_4 + (A_{66} + I_6)\ddot{\eta}_6 + B_{66}\dot{\eta}_6 = F_6 e^{i\omega t} \quad (3)$$

where η_2 is sway, η_4 roll, and η_6 yaw. A_{jk} and B_{jk} are the added-mass and damping coefficients, C_{jk} the restoring coefficients, and F_j the complex amplitudes of the wave exciting forces. ω is the wave-encounter frequency.

In keeping with the complex notation on the right-hand sides of the foregoing equations, the motion displacements η_k are assumed to be complex functions given by

$$\eta_k(t) = \eta_{ko} e^{i\omega t} = (\eta_{kR} + i\eta_{kI}) e^{i\omega t} \quad (4)$$

where η_{ko} is complex, but η_{kR} and η_{kI} are real. It is understood that in expressions involving complex variables, only the real

² Numbers in brackets designate References at end of paper.

part is physically realized. For example, in equation (4)

$$\eta_k(t) = \eta_{kR} \cos \omega t - \eta_{kI} \sin \omega t = \eta_{kA} \cos(\omega t + \theta_k) \quad (5)$$

where $\eta_{kA} = (\eta_{kR}^2 + \eta_{kI}^2)^{1/2}$ is amplitude and $\theta_k = \tan^{-1}(\eta_{kI}/\eta_{kR})$ is phase angle.

The A_{jk} , B_{jk} , C_{jk} , and F_j are ascribed the general forms:

$$\begin{aligned} A_{jk} &= A_{jk}^H + A_{jk}^F \\ B_{jk} &= B_{jk}^H + B_{jk}^F + B_{jk}^C \\ F_j &= F_j^H + F_j^F + F_j^C \end{aligned} \quad (6)$$

where superscript H denotes hull coefficients derived from strip theory, superscript F signifies contributions due to appendages (foils) such as rudders and fins, and superscript C denotes hull circulatory terms.

For B_{44} , the roll damping coefficient, there is an additional term, B_{44}^V , the viscous roll damping coefficient. This takes account of the viscous resistance to rolling of bilge keels, hull, rudder, and other appendages.

Detailed expressions for the terms on the right-hand side of equation (6) will now be given.

Hull coefficients derived from strip theory

Expressions are given below for A_{jk}^H , B_{jk}^H , C_{jk}^H , and F_j^H . These are based on the strip theory of Salvesen et al [1], and are similar to the comparable terms given by Lee and Curphy [2]. However, use of stability axes instead of translating earth axes results in simpler expressions for A_{26}^H , B_{26}^H , A_{66}^H and B_{66}^H . The transformations involved are discussed in Appendix 1.

Nomenclature

A_{jk} = added-mass coefficient	S = foil area	n_j = component of unit outward normal to hull
B = beam, also damping coefficient	T = draft	r = distance from bilge keel to CG
B_{BK} = bilge keel roll damping coefficient	U = ship speed	s = x-coordinate of foil midchord
B_E = eddy-making roll damping coefficient	V = superscript for viscous damping	x, y, z = coordinate system
B_F = foil viscous roll damping coefficient	a = wave amplitude	x_p = x-coordinate of center of area of hull underwater profile
B_H = hull viscous roll damping coefficient	a_{jk} = sectional added-mass	\hat{y} = foil rolling moment arm
B_{jk} = damping coefficient	a_p = foil added-mass	Γ = foil dihedral angle
C = superscript denoting hull circulation	b_{jk} = sectional wavemaking damping	α = foil angle of attack
CG = center of gravity	b = foil span	β_s = heading angle relative to sea direction
C_{jk} = restoring coefficient	b_k = bilge keel breadth	γ = linear function of k_w , $\rightarrow 1$ as $k_w \rightarrow 0$
C_L = lift coefficient	c = foil mean chord	ξ = wave slope
$C_{L\alpha}$ = lift curve slope	c_a = sectional area coefficient	η_2 = sway displacement
C_P = prismatic coefficient	d = sectional draft	η_4 = roll angle
$C(k)$ = circulation delay function	dl = element of length along girth	$\dot{\eta}_4$ = roll amplitude
C_x = hull cross section	$e_F = \exp(-k_w h)$	η_6 = yaw angle
F = superscript denoting foil contribution	$e_H = \exp(-k_w c_a d)$	θ_k = phase angle
F_j = exciting force or moment	f_j = sectional Froude-Kriloff force	ξ = variable of integration in longitudinal direction
\overline{GM} = metacentric height, corrected for internal free surfaces	g = gravitational acceleration	ρ = water density
$G(k)$ = gust function	h = foil mean depth	ϕ_j = two-dimensional section potential
H = superscript denoting hull contribution	h_{CG} = height of CG above waterplane	ω = frequency of encounter
I_4 = rolling moment of inertia	h_j = sectional diffraction force	ω_w = wave frequency
I_6 = yawing moment of inertia	k = reduced frequency = $0.5\omega c/U$	
L = foil lift, also length between perpendiculars	k_w = wave number	
	m = ship mass	
	n = roll decay coefficient	

$$A_{22}^H = \int_L a_{22} d\xi \quad (7)$$

$$B_{22}^H = \int_L b_{22} d\xi \quad (8)$$

$$A_{24}^H = \int_L a_{24} d\xi \quad (9)$$

$$B_{24}^H = \int_L b_{24} d\xi \quad (10)$$

$$A_{26}^H = \int_L a_{22} \xi d\xi \quad (11)$$

$$B_{26}^H = \int_L b_{22} \xi d\xi \quad (12)$$

$$A_{44}^H = \int_L a_{44} d\xi \quad (13)$$

$$B_{44}^H = \int_L b_{44} d\xi \quad (14)$$

$$C_{44} = mg\overline{GM} \quad (15)$$

$$A_{46}^H = \int_L a_{24} \xi d\xi \quad (16)$$

$$B_{46}^H = \int_L b_{24} \xi d\xi \quad (17)$$

$$A_{62}^H = A_{26}^H - UB_{22}^H/\omega^2 \quad (18)$$

$$B_{62}^H = B_{26}^H + UA_{22}^H \quad (19)$$

$$A_{64}^H = A_{46}^H - UB_{24}^H/\omega^2 \quad (20)$$

$$B_{64}^H = B_{46}^H + UA_{24}^H \quad (21)$$

$$A_{66}^H = \int_L a_{22} \xi^2 d\xi \quad (22)$$

$$B_{66}^H = \int_L b_{22} \xi^2 d\xi \quad (23)$$

$$F_j^H = \rho a \int_L (f_j + h_j) d\xi \quad j = 2, 4 \quad (24)$$

$$F_6^H = \rho a \int_L \left[(f_2 + h_2) \xi + \frac{U}{i\omega} h_2 \right] d\xi \quad (25)$$

$$f_j(x) = -g \exp(-ik_w x \cos \beta_s)$$

$$\times \int_{C_x} n_j \exp[k_w(z' + iy \sin \beta_s)] dl \quad (26)$$

$$h_j(x) = \omega_w \exp(-ik_w x \cos \beta_s) \int_{C_x} \phi_j(in_3 - n_2 \sin \beta_2) \times \exp[k_w(z' + iy \sin \beta_s)] dl \quad (27)$$

The foregoing integrations are over the length of the ship. In practice, the hull length is divided into approximately 20 sections and the two-dimensional added-mass (a_{jk}) and wave-making damping (b_{jk}) are computed for each section. a_{22} and b_{22} result from swaying motions, a_{44} and b_{44} apply to roll, while a_{24} and b_{24} are due to cross-coupling between sway and roll. a is wave amplitude, and f_j and h_j are the sectional incident and diffraction forces, respectively. The integrations for the evaluation of f_j and h_j are performed over the submerged hull section C_x . n_2 and n_3 are the y and z components of the unit outward normal to the hull at (x, y, z) , Fig. 1, and

$$n_4 = yn_3 - zn_2 \quad (28)$$

$$z' = z + h_{CG} \quad (29)$$

ϕ_2 and ϕ_4 are the two-dimensional section potentials for sway

and roll oscillations. ω_w is wave frequency and k_w is wave number, given by

$$k_w = \omega_w^2/g \quad (30)$$

h_{CG} is the height of the center of gravity above the water-plane, and β_s is the heading angle relative to the sea, defined in Fig. 2. ω_w is related to ω , the frequency of encounter, by

$$\omega = \omega_w - k_w U \cos \beta_s \quad (31)$$

Lifting surface contributions

When $U > 0$, hull appendages such as the rudder, skeg, and propeller shaft brackets act as lifting surfaces to generate both damping and exciting forces; the contribution to roll damping is especially significant. Of lesser importance are the appendage added-mass terms, which are independent of speed.

The lifting surface (foil) coefficients are derived by applying the same methodology as used by the author for hydrofoil ship motion prediction [3]. The resulting expressions for A_{jk}^F , B_{jk}^F and F_j^F are

$$A_{22}^F = \Sigma a_p \sin^2 \Gamma \quad (32)$$

$$B_{22}^F = \frac{1}{2} \rho U \Sigma S C_{L\alpha} C(k) \sin^2 \Gamma \quad (33)$$

$$A_{24}^F = -\Sigma a_p \sin \Gamma \hat{y} \quad (34)$$

$$B_{24}^F = -\frac{1}{2} \rho U \Sigma S C_{L\alpha} C(k) \sin \Gamma \hat{y} \quad (35)$$

$$A_{26}^F = \Sigma a_p s \sin^2 \Gamma = A_{62}^F \quad (36)$$

$$B_{26}^F = \frac{1}{2} \rho U \Sigma S C_{L\alpha} C(k) (s - c/4) \sin^2 \Gamma \quad (37)$$

$$A_{44}^F = \Sigma a_p \hat{y}^2 \quad (38)$$

$$B_{44}^F = \frac{1}{2} \rho U \Sigma S C_{L\alpha} C(k) \hat{y}^2 \quad (39)$$

$$A_{46}^F = -\Sigma a_p s \sin \Gamma \hat{y} = A_{64}^F \quad (40)$$

$$B_{46}^F = -\frac{1}{2} \rho U \Sigma S C_{L\alpha} C(k) \sin \Gamma (s - c/4) \hat{y} \quad (41)$$

$$B_{62}^F = \frac{1}{2} \rho U \Sigma x S C_{L\alpha} C(k) \sin^2 \Gamma \quad (42)$$

$$B_{64}^F = -\frac{1}{2} \rho U \Sigma x S C_{L\alpha} C(k) \sin \Gamma \hat{y} \quad (43)$$

$$A_{66}^F = \Sigma a_p s^2 \sin^2 \Gamma \quad (44)$$

$$B_{66}^F = \frac{1}{2} \rho U \Sigma S C_{L\alpha} C(k) (s - c/4) x \sin^2 \Gamma \quad (45)$$

$$F_2^F = a \Sigma f_2^F \quad (46)$$

$$F_4^F = a \Sigma f_4^F \quad (47)$$

$$F_6^F = a \Sigma f_2^F s \quad (48)$$

$$f_2^F = f_F \sin \Gamma$$

$$f_4^F = -f_F \hat{y}$$

$$f_F = -\omega_w (\sin \Gamma \sin \beta_s + i \cos \Gamma) \left(\frac{1}{2} \rho U S C_{L\alpha} G(k) + i \omega a_p \right) \times \exp[-k_w (h + i(x \cos \beta_s - y \sin \beta_s))] \quad (49)$$

Summation is over all foil elements, including rudder, skeg, fins, and propeller shaft brackets. Γ is the dihedral angle, for which the following sign convention is adopted [3]: Γ for port-side fins and brackets is illustrated in Fig. 3; note that for

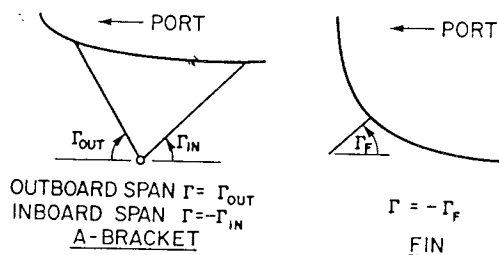


Fig. 3 Dihedral angle convention

these foil elements, $\Gamma(\text{starboard}) = -\Gamma(\text{port})$. For rudders and skegs, $\sin \Gamma = -1$.

The rolling moment arm is

$$\hat{y} = y \cos \Gamma + z \sin \Gamma \quad (50)$$

and a_p is the added-mass of a foil being accelerated perpendicular to its surface. For sufficiently large aspect ratios, such as the A-brackets, $a_p = \pi \rho b(c/2)^2$. For low-aspect-ratio foils, such as the rudder, empirical expressions should be used for a_p .

A small additional contribution to B_{44} is obtained by regarding the bilge keels as very-low-aspect-ratio lifting surfaces:

$$B_{BK}^F = \pi \rho U b_k^2 r^2 \quad (51)$$

where b_k is bilge keel breadth and r the distance from bilge keel to the CG.

The exciting force acting on an individual foil element is f_F . The methods given in reference [4] are used to evaluate $C(k)$, the circulation delay function, and $G(k)$, a modified form of Jones's gust function. k is the reduced frequency. a_p is included in equation (49) to account for the effect of wave orbital acceleration.

Viscous roll damping

The viscous roll damping coefficient may be expressed as follows:

$$B_{44}^V = B_{BK} + B_E + B_H + B_F \quad (52)$$

where B_{BK} , B_E , and B_H denote contributions from bilge keels, eddy-making resistance of the hull, and hull friction, respectively. B_F represents the viscous effect of appendages other than bilge keels (rudders, fins, etc.) at zero speed. Of the four components of B_{44}^V , B_{BK} is normally by far the largest.

Viscous roll damping is, of course, a nonlinear function of roll amplitude. A linear approximation is obtained by equating the energy dissipated by the nonlinear viscous effect during one roll cycle to that dissipated by a linear damping term. This is done as follows:

Denote by B the linear damping coefficient and let the roll angle be given by

$$\eta_4 = \hat{\eta}_4 \sin \omega t \quad (53)$$

where $\hat{\eta}_4$ is the roll amplitude. Now $B\hat{\eta}_4$ represents a torque about the CG and, during one roll cycle, the following amount of work must be done against this torque:

$$4 \int_0^{\hat{\eta}_4} B \hat{\eta}_4 d\eta_4 = 4\omega^2 B \int_0^{\pi/2\omega} \cos^2 \omega t dt = \pi \omega B \hat{\eta}_4^2 \quad (54)$$

If the energy dissipated by the viscous effect is E , then B is given by

$$B = \frac{E}{\pi \omega \hat{\eta}_4^2} \quad (55)$$

Bilge keels

The most complete study to date of the effect of bilge keels on ship rolling has been carried out by Kato [5], who found that the following factors influenced bilge keel effectiveness: bilge keel area, breadth and aspect ratio, Reynolds number, ship draft, distance from the bilge keel to the CG, height of the CG, and form of the bilge. After analyzing considerable experimental data, he devised the following empirical method for calculating the energy dissipated through bilge keel action.

The energy dissipated in one roll cycle is given by

$$E = 4 \rho l b_k r \hat{\eta}_4 (r \hat{\eta}_4 / T)^2 C_0 C_a C_k C_n \textcircled{B} F^{-\alpha} \quad (56)$$

Where l is the bilge keel length, b_k bilge keel breadth, r the distance from the center of the bilge keel to the CG, and T the period. C_0 , C_a , C_k , C_n , \textcircled{B} , and F are coefficients depending on ship form and Reynolds number.

A close look at equation (56) shows that a viscous force of the usual form,

$$F_V = \frac{1}{2} \rho V_R^2 S_{BK} C_{BK} \quad (57)$$

acts on the bilge keel with moment arm r about the CG. V_R is average velocity of the bilge keel due to roll, S_{BK} is bilge keel area, and C_{BK} is a drag coefficient. Equations to compute the various components of C_{BK} (C_0 , C_a , etc.) are given in Appendix 2.

From equations (55) and (56), the bilge keel damping coefficient is given by

$$B_{BK} = \frac{1}{\pi^3} \rho l b_k r^3 \omega \hat{\eta}_4 C_0 C_a C_k C_n \textcircled{B} F^{-\alpha} \quad (58)$$

In computing B_{BK} , the same approach is taken as in computing added-mass and wavemaking damping; that is, the sectional contributions are computed individually and then summed.

Eddy-making

The results of this section are due to Tanaka [6], who conducted rolling experiments with various ship sections to assess the effect of section shape on eddy-making roll damping.

The roll-resisting force due to eddy-making is expressed as

$$F = \frac{1}{2} \rho (r \hat{\eta}_4)^2 S C \quad (59)$$

where r is the distance from the CG to the point on the hull where the eddies are generated, S is wetted surface area of the hull section, and C is a drag coefficient depending on hull form.

Now F exerts a torque about the CG given by

$$T = Fr = \frac{1}{2} \rho r^3 S C \hat{\eta}_4^2 \omega^2 \cos^2 \omega t \quad (60)$$

The energy dissipated by this torque during one roll cycle is

$$E = 4 \int_0^{\hat{\eta}_4} T d\eta_4 = \frac{4}{3} \rho r^3 \hat{\eta}_4^3 \omega^2 S C \quad (61)$$

whence, from (55), the eddy-making damping coefficient is

$$B_E = \frac{4}{3\pi} \rho \omega \hat{\eta}_4 r^3 S C \quad (62)$$

It remains to evaluate C . Empirical expressions for C as a function of section shape are given in Appendix 3.

Hull friction

In Appendix 4 it is shown that the hull frictional damping coefficient is given by

$$B_H = \frac{4}{3\pi} \rho \omega \hat{\eta}_4 C_{DF} \int_L dx \int_{C_x} r (y n_2 + z n_3)^2 dl \quad (63)$$

where C_{DF} is the skin friction drag coefficient, C_x a hull cross section, dl a girthwise length element, and

$$r = (y^2 + z^2)^{1/2} \quad (64)$$

If forward speed U is nonzero, the Schoenherr line based on smooth turbulent flow is used to evaluate C_{DF} :

$$C_{DF} = 0.0004 + \left(3.46 \log \left(\frac{UL}{\nu} \right) - 5.6 \right)^{-2} \quad (65)$$

where 0.0004 is the standard roughness correction and ν is kinematic viscosity. Note that the Reynolds number is based on forward speed, U , and the length between perpendiculars, L .

If $U = 0$, C_{DF} is evaluated by the following method, due to Kato [7]:

$$C_{DF} = 1.328R_n^{-0.5} + 0.014R_n^{-0.114} \quad (66)$$

$$R_n = \frac{3.22}{T\nu} (\bar{r}\hat{\eta}_4)^2 \quad \text{PERIOD} \quad (67)$$

$$\bar{r} = \frac{1}{\pi} \{ (0.887 + 0.145C_B)(1.7T + BC_B) + 2(\overline{KG} - T) \} \quad (68)$$

where C_B is the block coefficient, \overline{KG} the height of the CG above the keel, B the ship beam, and T the draft. R_n is a Reynolds number based on average rolling velocity and average distance from the CG, \bar{r} .

Appendages other than bilge keels

At zero forward speed, viscous drag forces opposing roll act on appendages such as rudders and fins. By regarding these as oscillating flat plates and applying the method described by equations (53) to (55), we obtain the following expression for the appendage viscous roll damping coefficient:

$$B_F = \frac{4}{3\pi} \rho \omega \hat{\eta}_4 \Sigma (y^2 + z^2)^{3/2} S C_n \quad (69)$$

where summation is over all foil elements. C_n is the normal-force coefficient for a flat plate inclined at a large angle to the flow; Hoerner [8] gives a value of 1.17 for C_n when the angle of inclination exceeds 40 deg.

Hull circulatory effects

The hull circulatory terms (B_{jk}^C , F_j^C) are evaluated following the methods given by Mandel [9]. Let

$$B_C = \frac{\pi}{2} \rho U T^2 \quad (70)$$

where T is draft. Then

$$B_{22}^C = B_C \quad (71)$$

$$B_{26}^C = B_C x_p = B_{62}^C \quad (72)$$

$$B_{66}^C = B_C \left(\frac{1}{2} C_P L \right)^2 + U \int_L a_{22} \xi d\xi \quad (73)$$

where x_p is the x -coordinate of the center of area of the hull underwater profile and C_P is the prismatic coefficient.

The action on the hull of the horizontal component of wave orbital velocity generates contributions to the sway and yaw exciting forces. These are estimated by assuming that the hull is a wing with chord L and span varying with sectional draft, and, further, that lift is uniformly distributed along the ship's length. The resulting terms are

$$f_2^C = -\omega_w T_x \sin \beta_s \exp[-k_w(ix \cos \beta_s + T_x/2)] \quad (74)$$

$$F_2^C = a \frac{B_C}{S_p} \int_L f_2^C dx \quad (75)$$

$$F_6^C = a \frac{B_C}{S_p} \int_L f_2^C x dx \quad (76)$$

where T_x is section draft and S_p the horizontally projected area of the underwater hull.

Lateral motions in long waves

It is difficult to obtain from the foregoing mathematics a physical appreciation of the theoretical model; in particular, the expressions for the hull exciting forces are rather abstract in appearance. However, when wavelengths are long compared with the ship's beam, fairly simple approximations may be derived for the forcing functions. These approximations provide the basis for further theoretical analysis of the lateral motion problem. This study leads to instructive insight into the relative significance of the various terms in the equations of motion, particularly for the classical beam-sea problem.

Approximations for the forcing functions

Approximations valid for waves long relative to ship beam are derived in Appendix 5 for the hull and foil forcing functions. The fundamental approximations invoked are:

1. The term $\exp(k_w z')$ in the integral for the sectional incident and diffraction forces, equations (26) and (27), is replaced by $e_H = \exp(-k_w c_a d)$, where c_a and d are sectional area coefficient and draft, respectively.

$$2. \exp(ik_w y \sin \beta_s) = 1 + ik_w y \sin \beta_s$$

The results are

$$f_2 = -ie_H k_w g \sin \beta_s \exp(-ik_w x \cos \beta_s) A_x \quad (77)$$

$$f_4 = ie_H k_w g \sin \beta_s \exp(-ik_w x \cos \beta_s) M_x \quad (78)$$

$$h_j = -\frac{e_H}{\rho} \omega_w \sin \beta_s \exp(-ik_w x \cos \beta_s) \{ \gamma_j (b_{2j} + i\omega a_{2j}) + k_w (b_{4j} + i\omega a_{4j}) \} \quad (79)$$

$$f_j^F = -e_F \omega_w \sin \beta_s \exp(-ik_w x \cos \beta_s) \{ \gamma_F (b_{2j}^F + i\omega a_{2j}^F) + k_w (b_{4j}^F + i\omega a_{4j}^F) \} \quad (80)$$

where A_x and M_x are sectional area and roll-restoring moment, respectively. γ_j and γ_F are linear functions of k_w , of the general form $\gamma = 1 - dk_w$, where $h_{CC} \leq \bar{d} \leq h_{CC} + T$. a_{jk}^F and b_{jk}^F are the contributions of individual foil elements to A_{jk}^F and B_{jk}^F , respectively. $e_F = \exp(-k_w h)$.

The complex integrals in the complete expressions for the sectional exciting forces, equations (26) and (27), have been replaced by terms involving $\sin \beta_s$ and section area, moment, added mass, and damping. Analogous expressions have been derived for the foil exciting forces.

Further simplifications result in beam seas, $\beta_s = 90$ deg and $\omega_w = \omega$. Equations (77) to (80) become

$$f_2 = -ie_H k_w g A_x \quad (81)$$

$$f_4 = ie_H k_w g M_x \quad (82)$$

$$h_j = -\frac{e_H}{\rho} \omega \{ \gamma_j (b_{2j} + i\omega a_{2j}) + k_w (b_{4j} + i\omega a_{4j}) \} \quad (83)$$

$$f_j^F = -e_F \omega \{ \gamma_F (b_{2j}^F + i\omega a_{2j}^F) + k_w (b_{4j}^F + i\omega a_{4j}^F) \} \quad (84)$$

Denote by F_{ij} and H_j the total wave incident and diffraction forces, respectively, that is, the integrals over ship length of the sectional forces. Substitution of (81) to (83) into (24) and (25), and evaluation of the integrals, yields

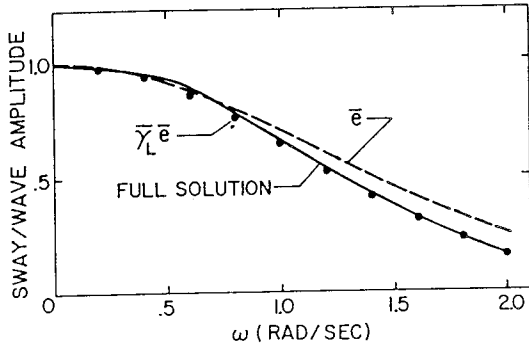


Fig. 4 Frigate, sway response in beam seas

$$F_{12} = -i\bar{e}mgk_w a \quad (90)$$

$$F_{14} = i\bar{e}mg\overline{GM}_S k_w a \quad (91)$$

$$F_{16} = 0 \quad (92)$$

$$H_2 = -\bar{e}\omega[\bar{\gamma}(B_{22}^H + i\omega A_{22}^H) + k_w(B_{24}^H + i\omega A_{24}^H)]a \quad (93)$$

$$H_4 = -\bar{e}\omega[\bar{\gamma}(B_{24}^H + i\omega A_{24}^H) + k_w(B_{44}^H + i\omega A_{44}^H)]a \quad (94)$$

$$I_6 = -\bar{e}\omega \left\{ \bar{\gamma} \left[B_{26}^H + i\omega A_{26}^H + \frac{U}{i\omega} (B_{22}^H + i\omega A_{22}^H) \right] + k_w \left[B_{46}^H + i\omega A_{46}^H + \frac{U}{i\omega} (B_{24}^H + i\omega A_{24}^H) \right] \right\} a \quad (95)$$

where \bar{e} and $\bar{\gamma}$ are mean values of e_H and γ_j . Note that \overline{GM}_S in equation (91) takes no account of internal free surfaces and that use of the CG as origin results in $F_{16} = 0$.

As regards the foil exciting forces, substitution of (84) into (46) to (48) yields the general result

$$F_j^F = -\bar{e}\omega[\bar{\gamma}(B_{2j}^F + i\omega A_{2j}^F) + k_w(B_{j4}^F + i\omega A_{j4}^F)]a \quad (96)$$

Finally, the hull circulation equations (74) to (76) yield

$$F_j^C = -\bar{e}\omega B_{2j}^C a \quad (97)$$

Note that it has now been assumed that $e_H = e_F = \bar{e}$ and that $\gamma_j = \gamma_F = \bar{\gamma}$.

Equations (90) to (97) are much simpler in form than the general expressions for the exciting forces, and provide the basis for further analysis of lateral motions in beam seas.

Lateral motions in beam seas of long wavelength

Specific consideration of beam seas of long wavelength yields considerable insight into the ship lateral motion problem. This is important from both a theoretical and a practical viewpoint since

- classical treatment of ship lateral motions generally concentrates on rolling in beam seas, and
- for ships of moderate to high metacentric height, rolling is greatest for seas on the beam.

Use will now be made of equations (90) to (97) to study lateral motions in beam seas of long wavelength, beginning with sway. In considering the sway equation, the roll and yaw coupling terms will be ignored, on the basis of the following reasoning.

The roll-to-sway coupling terms are $A_{24}\eta_4$ and $B_{24}\dot{\eta}_4$; note that in common with all wavemaking damping terms, B_{24}^H , the dominant component of B_{24} , $\rightarrow 0$ as $\omega \rightarrow 0$. Now when

waves are long relative to ship beam, both intuition and experience show that $\eta_4 = O(\bar{\zeta})$, where

$$\bar{\zeta} = k_w a \quad (98)$$

is wave slope. Hence the roll-to-sway coupling terms are both $O(\omega^4)$, and are negligible relative to F_2 , which is $O(\omega^2)$.

The argument for neglect of yaw-to-sway coupling follows similar lines, since both intuition and experience suggest that yaw is much smaller than roll in beam seas.

Without the roll and yaw terms and with the asymptotic expressions for F_2 , equation (1) becomes

$$[-\omega^2(A_{22} + m) + i\omega B_{22}]\eta_2 = [F_{12} + H_2 + F_2^F + F_2^C]e^{i\omega t} = \bar{e}a\{-imgk_w - \omega[\bar{\gamma}(B_{22} + i\omega A_{22}) + k_w(B_{24} + i\omega A_{24})]\}e^{i\omega t} \quad (99)$$

Upon retaining terms up to $O(\omega^2)$, the right-hand side (RHS) becomes

$$\bar{e}a[-\omega^2(A_{22} + m) + i\omega B_{22}]e^{i\omega t} \quad (100)$$

Thus sway phase leads wave phase by 90 deg and, as $\omega \rightarrow 0$, sway amplitude \rightarrow wave amplitude.

Figure 4 demonstrates that equation (100) gives a good approximation of sway response in beam seas, especially at low wave frequencies. The data plotted apply to a frigate at cruise speed. The solid line is the result of solving the full equations of motion while the dashed line is equation (100) with $\bar{e} = \exp(-k_w C_M T)$, where C_M is the midship sectional-area coefficient. The validity of neglecting coupling of roll and yaw into sway is clearly demonstrated.

The approximation (100) for sway response may be further improved by multiplying the RHS by

$$\bar{\gamma}_L = 1 - h_{CC}k_w \quad (101)$$

to give

$$\eta_2 = i\bar{e}\bar{\gamma}_L a e^{i\omega t} \quad (102)$$

Figure 4 demonstrates that equation (102) is a very good approximation for sway response over the entire frequency range of interest.

Consider next roll and ignore yaw coupling. From equation (2) with the approximation (102) for η_2

$$[-\omega^2(A_{44} + I_4) + i\omega B_{44} + C_{44}]\eta_4 = [F_{14} + H_4 + F_4^F - i\bar{e}\bar{\gamma}_L a(-\omega^2 A_{24} + i\omega B_{24})]e^{i\omega t} = \bar{e}a\{img\overline{GM}_S k_w - \omega[(B_{24} + i\omega A_{24})(\bar{\gamma} - \bar{\gamma}_L) + k_w(B_{44} + i\omega A_{44})]\}e^{i\omega t} \quad (103)$$

We now neglect the term involving $(\bar{\gamma} - \bar{\gamma}_L)$. Note that this is the same as assuming

$$|\bar{T}(B_{24} + i\omega A_{24})| \ll |B_{44} + i\omega A_{44}|$$

where \bar{T} lies between 0 and T . This is a reasonable assumption for normal hull forms. With this approximation, equation (103) becomes

$$[-\omega^2(A_{44} + I_4) + i\omega B_{44} + C_{44}]\eta_4 = i\bar{e}\bar{\zeta}(mg\overline{GM}_S - \omega^2 A_{44} + i\omega B_{44}) \quad (104)$$

Thus, sway coupling into roll cancels both the foil exciting moment and the primary component of the hull diffraction moment. The result is an uncoupled equation very similar in form to that derived by Conolly [10] on an intuitive basis. The use of such an uncoupled equation to predict roll is discussed extensively by Cox and Lloyd [11].

As $\omega \rightarrow 0$, $\eta_4 \rightarrow i\bar{\zeta}(\overline{GM}_S/\overline{GM})e^{i\omega t}$. Thus, roll amplitude

approaches wave slope, factored by the ratio of solid-to-liquid metacentric height, and roll phase leads wave phase by 90 deg.

Consider finally the yaw equation. From equation (3) with η_2 given by (102)

$$\begin{aligned} & [-\omega^2(A_{66} + I_6) + i\omega B_{66}]\eta_6 + (-\omega^2 A_{64} + i\omega B_{64})\eta_4 \\ & = [H_6 + F_6^F + F_6^C - i\bar{e}\bar{\gamma}_L a(-\omega^2 A_{62} + i\omega B_{62})]e^{i\omega t} \\ & = -\bar{e}\omega a \left\{ (\bar{\gamma} - \bar{\gamma}_L) \left[B_{26} \right. \right. \\ & \quad \left. \left. + i\omega A_{26} + \frac{U}{i\omega} (B_{22}^H + i\omega A_{22}^H) \right] \right. \\ & \quad \left. + k_w \left[B_{46} + i\omega A_{46} + \frac{U}{i\omega} (B_{24}^H + i\omega A_{24}^H) \right] \right\} e^{i\omega t} \quad (105) \end{aligned}$$

If, as for roll, the term involving $(\bar{\gamma} - \bar{\gamma}_L)$ is neglected, the RHS becomes

$$-\bar{e}\omega\bar{\zeta} \left[B_{46} + i\omega A_{46} + \frac{U}{i\omega} (B_{24}^H + i\omega A_{24}^H) \right] e^{i\omega t}$$

Thus, sway coupling into yaw cancels the primary components of the yaw exciting moment, leaving the latter of the same order as the roll-to-yaw coupling terms, that is, $O(\omega^3)$. Because yawing inertia and damping are very large, yaw is consequently virtually negligible in beam seas. This conclusion may be reinforced by substituting the asymptotic expression $i\bar{e}\bar{\zeta}e^{i\omega t}$ for η_4 , whereupon the yaw equation becomes

$$\begin{aligned} & [-\omega^2(A_{66} + I_6) + i\omega B_{66}]\eta_6 \\ & = -\bar{e}\omega\bar{\zeta} \left[B_{46} + i\omega A_{46} + \frac{U}{i\omega} (B_{24}^H + i\omega A_{24}^H) \right. \\ & \quad \left. - i\omega A_{64} - B_{64} \right] = 0 \quad (106) \end{aligned}$$

So at low frequencies, sway and roll coupling into yaw completely cancel F_6 . Note, however, that if $\overline{GM}_S > \overline{GM}$, roll-to-yaw coupling gives some net yaw excitation.

Roll damping

Good estimates of roll damping are essential for solving the roll prediction problem, particularly in beam seas where for long wavelengths equation (104) demonstrates that rolling dynamics reduce to a simple second-order system. It is instructive to rewrite this equation in the conventional form [11]:

$$\eta_4 = \left[\frac{\omega_0^2 - \omega^2 q + 2in\omega_0\omega}{\omega_0^2 - \omega^2 + 2in\omega_0\omega} \right] \bar{\zeta} e^{i\omega t} \quad (107)$$

where

$$\omega_0 = \left(\frac{C_{44}}{A_{44} + I_4} \right)^{1/2} \quad (108)$$

is roll natural frequency

$$q = A_{44}/(I_4 + A_{44}) \quad (109)$$

is the ratio of hydrodynamic moment of inertia to total moment of inertia, and

$$n = \frac{B_{44}}{2\omega_0(A_{44} + I_4)} = \frac{\omega_0 B_{44}}{2C_{44}} \quad (110)$$

is roll decay coefficient. For convenience, it is assumed that $\overline{GM}_S = \overline{GM}$.

At resonance ($\omega = \omega_0$), equation (107) gives

$$\frac{\eta_4}{\bar{\zeta}} = \left(\frac{1 - q + 2in}{2in} \right) e^{i\omega t} \quad (111)$$

which illustrates the importance of an accurate estimate of n , as this parameter determines peak response in beam seas.

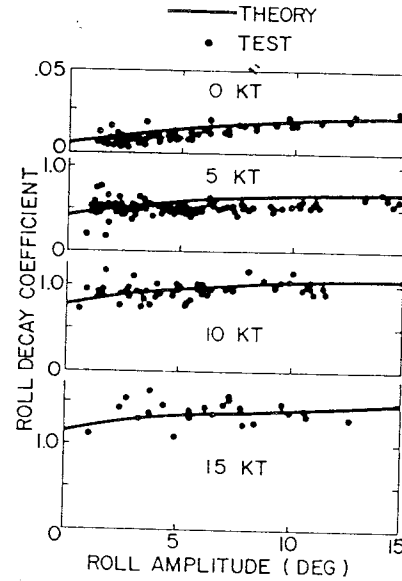


Fig. 5 FFG-7 model, roll decay coefficient

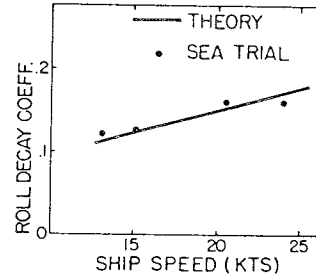


Fig. 6 Frigate, roll decay coefficient

That the present theory does give reasonable estimates of roll damping is demonstrated in Figs. 5 and 6, where theoretical predictions of n are compared with experimental values for two different warship hull forms of frigate size. The data in Fig. 5 were obtained from calm-water experiments with a 1:20.8-scale self-propelled model of the guided-missile frigate, FFG-7 [12], while the data in Fig. 6 were measured during full-scale forced-rolling trials [10] of a Royal Navy frigate. Particulars on the hull forms are given in the references.

In Fig. 5, n is plotted against initial angle of roll for speeds of 0, 5, 10, and 15 knots. The measurements were obtained by inclining the model to an initial roll angle, then releasing it and measuring the resulting roll decay characteristics. A large number of measurements were taken, and the resulting scatter gives a good idea of the experimental variability. Theory is in good agreement with the measurements at all four speeds shown. Especially noteworthy is the fact that the rapid increase in damping with increasing speed is well predicted. For the FFG-7, by far the greatest portion of this damping at nonzero speed results from the large spade rudder mounted directly behind the propeller. In making the theoretical estimates, the effects of propeller slipstream were accounted for using the procedure suggested by Barr and Ankudinov [13].

The ship of Fig. 6 is equipped with fin stabilizers, which were employed in the trials to build up large roll angles that were then allowed to decay naturally with the fins locked in the mean position. The resulting measurements of n are plotted against speed, together with the theoretical estimates. Again, agreement between theory and experiment is good.

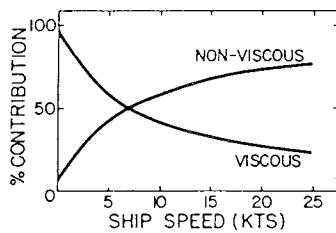


Fig. 7 Frigate, roll damping components with twin rudders, one pair of fins

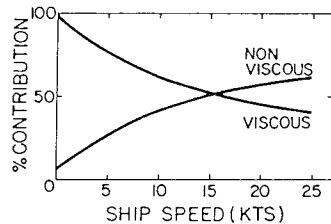


Fig. 8 Destroyer, roll damping components with single rudder, no fins

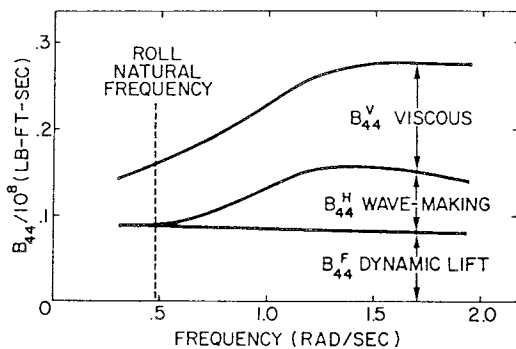


Fig. 9 Destroyer, roll damping components at 20 knots

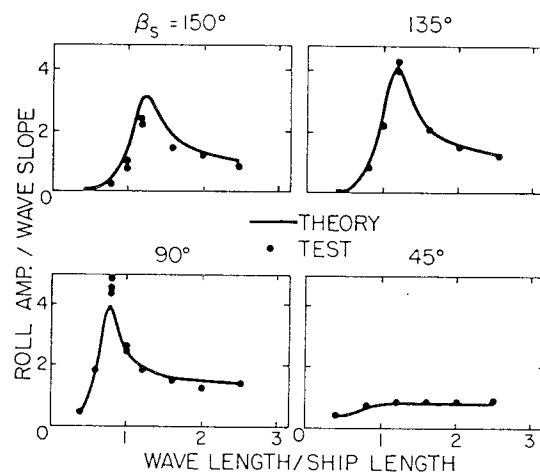


Fig. 10 Frigate model, heading effect, $F_n = 0.15$, BK_1, GM_1

Comparison of theory with experiment

Experimental data for comparison with theory have been obtained from four sources: regular wave tests [14] with a fully appended self-propelled frigate model at the seakeeping basin of the David W. Taylor Naval Ship Research and Development Center (DTNSRDC), sea trials [15] of the oceanographic research ship CFAV *Quest*, sea trials [10] of the same ship for which roll damping data are given in Fig. 6, and sea trials of a Canadian destroyer. Only roll data are presented, since measurements of sway and yaw are virtually nonexistent.

Figures 10 to 14 present extensive experimental data for the frigate model tested at DTNSRDC. This was a comprehensive experimental program in which metacentric height, bilge keel configuration, heading, and forward speed were systematically varied. Two different bilge keels were used (designated BK_1 and BK_3) and three metacentric heights (GM_1 , GM_2 and GM_3). Some details are as follows:

Length between perpendiculars	5.54 m (18.182 ft)	
Beam	0.66 m (2.156 ft)	
Draft	0.22 m (0.716 ft)	
Block coefficient	0.485	
Prismatic coefficient	0.604	
Metacentric height designation	percent of beam	
GM_1	12.1	
GM_2	9.0	
GM_3	6.1	
Bilge keel designation	Area in percent of wetted area	Length in percent of LBP
BK_1	2.34	29.6
BK_3	1.00	17.0

Figures 10 and 11 show the effect on roll response of varying sea direction at low and high Froude numbers, respectively. Figures 12 and 13 show the effect of varying metacentric height and bilge keel configuration at low Froude number in bow seas and high Froude number in beam seas. Finally, Fig. 14 presents data showing the influence of metacentric height on roll response in quartering seas at low Froude number.

Agreement between theory and experiment is generally very good. The following points are especially worthy of mention:

1. The considerable variation in roll response with heading to the sea is reasonably well predicted, both at low and high speed.
2. Predictions of peak response are generally good, indicating good estimation of roll damping.

The importance of including dynamic lift on appendages in predicting roll damping has already been mentioned. Figures 7 and 8 illustrate this point, giving a theoretical breakdown of B_{44} between viscous (B_{44}^V) and nonviscous ($B_{44}^H + B_{44}^F$) contributions. Recall that B_{44}^V , B_{44}^F , and B_{44}^H are, respectively, the viscous, foil dynamic lift, and hull wavemaking components of roll damping. All damping components are evaluated at the roll natural frequency, to which the data in Fig. 9 apply, wavemaking damping is relatively low.

The dominance of the nonviscous contribution at cruise speeds is readily apparent. Further, for both ships the nonviscous portion results almost entirely from dynamic lift. Figure 9 illustrates this point for the destroyer, giving a plot of roll damping components at a speed of 20 knots. At the roll natural frequency, to which the data in Fig. 9 apply, wavemaking damping is relatively low. Figures 7 to 9 clearly show that it is essential to include dynamic lift in theoretical estimates of roll damping. Without this effect, damping will be significantly underpredicted at even moderate speeds.

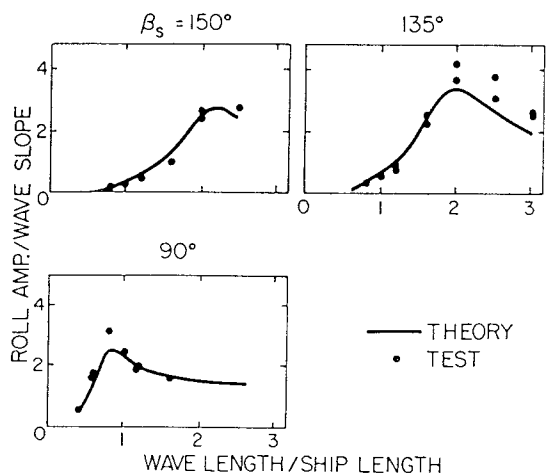


Fig. 11 Frigate model, heading effect, $F_n = 0.46$, $BK_1 GM_1$

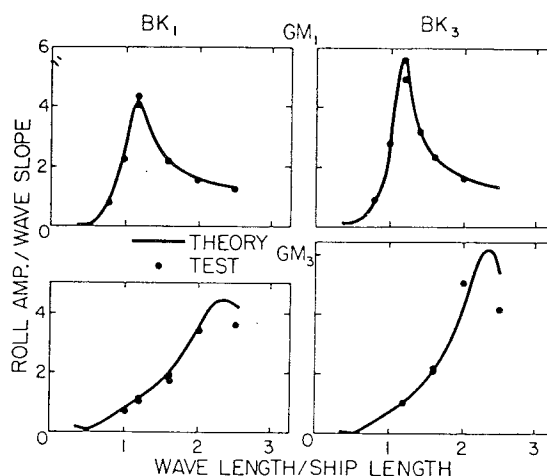


Fig. 12 Frigate model, GM effect, $F_n = 0.15$, bow seas

3. Theory correctly predicts a substantial reduction in roll response as speed increases. This decrease is mainly due to the twin rudders, which contribute significantly to roll damping at high speed.

4. The dramatic increase in roll response in quartering seas as metacentric height is reduced is very well predicted. This is of considerable practical importance, since the GM_3 case is representative of the metacentric height/beam ratio at which frigates and destroyers commonly operate.

Figures 15 and 16 present sea trials data for CFAV *Quest*, for which the leading particulars are [15]:

Displacement during trials	2255 tons (2291 metric tons [t])
Length between perpendiculars	234 ft (71.3 m)
Beam	42 ft (12.8 m)
Draft	16 ft (4.8 m)

Figure 15 compares computed and measured roll response at 0 and 10 knots. The experimental points were obtained from roll and wave spectra measured during the trials, simultaneously in the case of zero speed. Agreement between theory and measurement is good, particularly since the measurements come from full-scale sea trials with attendant uncertainties in wave direction and spectral measurement. Again the decrease in peak response with increasing speed is correctly predicted.

Figure 16 shows that when the theoretical beam sea roll responses given in Fig. 15 are applied to the wave spectra measured during the trials, a good estimate of root-mean-square (rms) roll angle is obtained. Data are also given in Fig. 16 for the bow and quartering sea directions, and again reasonable agreement is demonstrated, even though the theoretical calculation has been performed for a long-crested sea.

Figures 17 and 18 make further comparisons of theory with full-scale measurements of roll response on two different ships. As for the *Quest* results in Fig. 15, the experimental points were derived from roll and wave spectra measured during the trials.

The experimental data in Fig. 17 have been published by Conolly [10]. Some ship particulars are listed in the following; note the presence of a single pair of fin stabilizers, which were locked in the mean position during the trials:

Displacement during trials	2540 t (2500 tons)
Length between perpendiculars	106.7 m (350 ft)

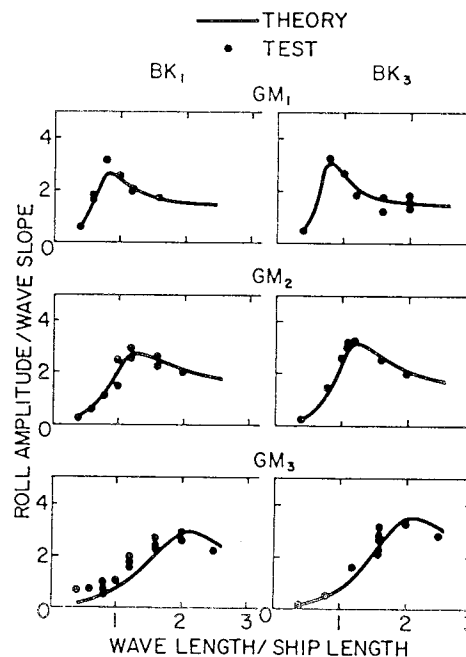


Fig. 13 Frigate model, GM effect, $F_n = 0.46$, beam seas

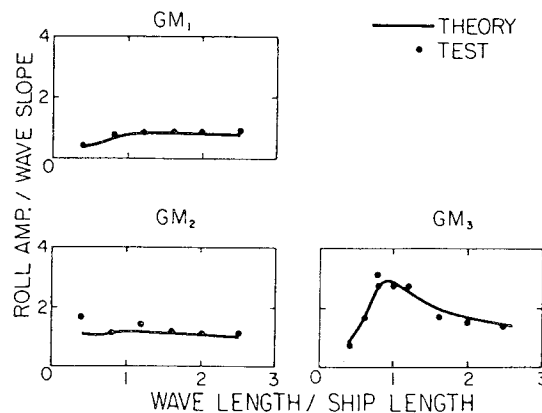


Fig. 14 Frigate model, GM effect, $F_n = 0.15$, quartering seas

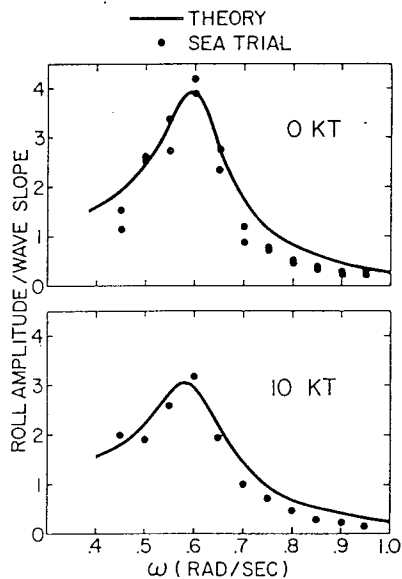


Fig. 15 CFAV Quest, roll response in beam seas

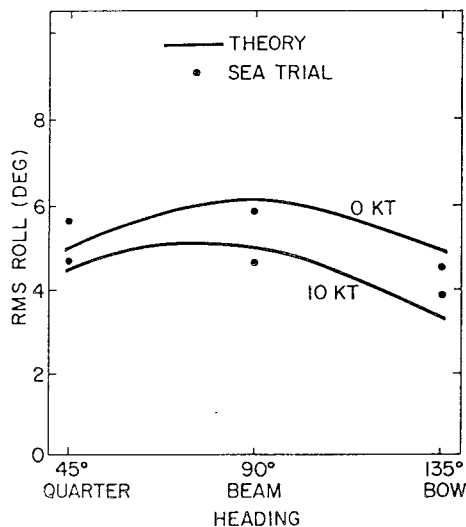


Fig. 16 CFAV Quest, rms roll versus heading

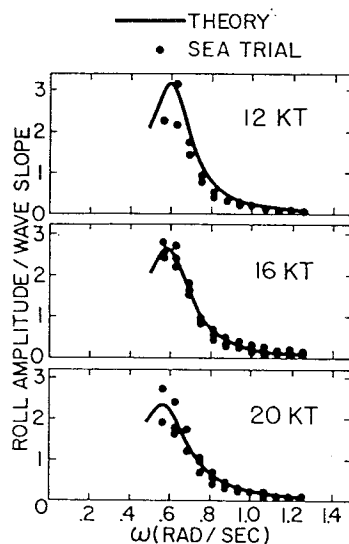


Fig. 17 Frigate, roll response in beam seas

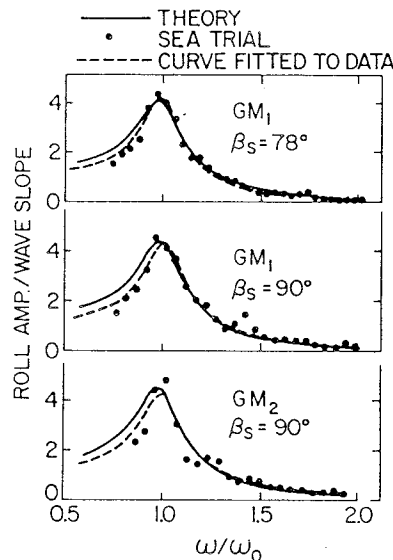


Fig. 18 Destroyer, roll response in beam seas, 10 knots

beam	13.1 m (43 ft)
Draft	3.7 m (12 ft)
stabilizer fin area	2.6 m ² (28 ft ²)

Results are given in Fig. 17 for beam seas and three speeds 12, 16, and 20 knots). Three sets of measurements were obtained at 16 and 20 knots, and two at 12 knots. Agreement between theory and experiment is good, particularly at the two higher speeds.

Finally, Fig. 18 presents roll response data obtained from sea trials with a Canadian destroyer conducted and analyzed by Miles [16]. Some ship particulars are:

Displacement full load	4267 t (4200 tons)
Length between perpendiculars	121.3 m (398 ft)
Beam	15.2 m (50 ft)
Draft	4.4 m (14.5 ft)

Results are given in Fig. 18 for a speed of 10 knots, two sea directions (78 and 90 deg), and two metacentric heights (where $\bar{M}_1 = 1.1 GM_2$). In addition to the theoretical predictions

(solid lines) and data points, curves fitted to the data by Miles [16] are also plotted (dashed lines). These are of the form

$$\eta_{4A} = C_1 \exp(-C_2 \omega^2) / [(C_1 - \omega^2)^2 + C_3 \omega^2]^{1/2}$$

where C_1 , C_2 , and C_3 are constants for a given set of response data.

The agreement between theory and the experimental points is very good near resonance and above. Below resonance, theory overpredicts roll response, but Miles notes that the accuracy of the wave measurement is suspect at such low frequencies. The close agreement of theory with the curves fitted to the data is also noteworthy.

Comparisons of predicted and measured rms roll angle are made in the following, with the results expressed as a ratio of theory/measurement. The theoretical estimation makes use of the wave spectra measured during the trials in conjunction with the response transforms of Fig. 18. It is assumed that the seas are long crested. Correlation is very good for all three runs.

\overline{GM}	β_s	Theory/ Measurement
1	78 deg	1.05
1	90 deg	0.97
2	90 deg	0.97

In view of the correlation shown above and in Fig. 16 between predicted and measured rms roll, which has been achieved using long-crested seas in the theoretical calculation, it is suggested that the occurrence of long-crested seas should not be ignored in making full-scale seakeeping predictions.

Conclusion

A theoretical model has been presented for the prediction of ship sway, roll, and yaw motions in oblique waves. In this model hull exciting forces, added-mass, and wavemaking damping are computed by the usual means of strip theory. Upon these are superposed linearized terms to account for dynamic lift on appendages and hull. Viscous roll damping is taken into account using empirical formulations based on model test data.

The behavior of the theoretical model has been examined for waves that are long relative to ship beam. Reasonably simple approximations have been derived for this case for the hull and foil forcing functions. Using these, the classical problem of lateral motions in beam seas has been analyzed, and the principal results of this analysis are summarized as follows. It is emphasized that these apply rigorously only to beam seas of low frequency.

1. Sway coupling into roll cancels both the foil exciting moment and the primary component of the hull diffraction moment. As a result, rolling is described by a single equation very similar in form to that derived by Conolly on an intuitive basis.

2. Roll and yaw coupling into sway are negligible. Sway response is well approximated by an exponential decay with a 90 deg phase lead.

3. The net yawing moment due to the incident wave forces is negligible; furthermore, sway coupling into yaw cancels the primary components of the remainder of the yaw exciting moment. What remains is of the same order as the roll-to-yaw coupling terms. Yaw amplitudes are consequently very small.

Roll damping has been discussed, and it has been demonstrated that the model makes reasonable estimates of this most critical coefficient. Examples have been presented showing the relative significance of the viscous, dynamic lift, and hull wavemaking components of roll damping. These demonstrate that at moderate and high speeds, it is essential to include dynamic lift in theoretical estimates of roll damping; without this effect, damping will be significantly underpredicted.

Extensive comparisons of predicted and measured roll response have been presented, using both model and full-scale data, with generally very satisfactory correlation. The following points are especially noteworthy.

1. Predictions of peak response are generally good, indicating good estimation of roll damping. This is particularly true of the full-scale comparisons.

2. Theory correctly predicts a substantial reduction in roll response as speed increases. This decrease is due to dynamic lift effects.

3. The considerable variation in roll response with heading to the sea is reasonably well predicted.

4. For two of the full-scale sea trials, rms roll angle has been well estimated using long-crested seas in the theoretical calculation. This suggests that the occurrence of long-crested seas should not be ignored in making full-scale seakeeping predictions.

On the basis of the correlation studies, it is concluded that the theoretical model predicts roll with roughly the same accuracy as standard seakeeping computer programs predict pitch and heave. It must be pointed out, however, that to achieve good roll predictions, considerably more information must be supplied than is required for pitch-heave predictions; in particular, appendages must be specified in some detail because of their dominant contribution to roll damping.

References

- 1 Salvesen, N., Tuck, E. O., and Faltnsen, O., "Ship Motions and Sea Loads," TRANS. SNAME, Vol. 78, 1970.
- 2 Lee, C. M. and Curphey, R. M., "Prediction of Motion, Stability, and Wave Load of Small-Waterplane-Area, Twin-Hull Ships," TRANS. SNAME, Vol. 85, 1977.
- 3 Schmitke, R. T., "Prediction of Wave-Induced Motions for Hullborne Hydrofoils," *Journal of Hydronautics*, Vol. 11, 1977.
- 4 Drummond, T. G., Mackay, M., and Schmitke, R. T., "Wave Impacts on Hydrofoil Ships and Structural Implications," *Proceedings, Eleventh Symposium on Naval Hydrodynamics*, London, 1976.
- 5 Kato, H., "Effect of Bilge Keels on the Rolling of Ships," *Memories of the Defence Academy*, Japan, Vol. 4, 1966.
- 6 Tanaka, N., "A Study on the Bilge Keels (Part 4—On the Eddy-Making Resistance to the Rolling of a Ship Hull)," *Journal of the Society of Naval Architects of Japan*, Vol. 109, 1960.
- 7 Kato, H., "On the Frictional Resistance to the Roll of Ships," *Journal of the Society of Naval Architects of Japan*, Vol. 102, 1958.
- 8 Hoerner, S. F., *Fluid Dynamic Drag*, published by the author, 1958.
- 9 Mandel, P., "Ship Maneuvering and Control," in *Principles of Naval Architecture*, J. P. Comstock, Ed., SNAME, 1967.
- 10 Conolly, J. E., "Rolling and Its Stabilization by Active Fins," *Trans. RINA*, Vol. 111, 1969.
- 11 Cox, G. G. and Lloyd, A. R., "Hydrodynamic Design Basis for Navy Ship Roll Motion Stabilization," TRANS. SNAME, Vol. 85, 1977.
- 12 Jones, H. D. and Cox, G. G., "Roll Stabilization Investigation for the Guided Missile Frigate (FFG-7)," DTNSRDC Ship Performance Department Report SPD-495-18, July 1976.
- 13 Barr, R. A. and Ankudinov, V., "Ship Rolling, Its Prediction and Reduction Using Roll Stabilization," *Marine Technology*, Vol. 14, 1977.
- 14 Baitis, A. E. and Wermter, R., "A Summary of Oblique Sea Experiments Conducted at the Naval Ship Research and Development Center," 13th International Towing Tank Conference, 1972.
- 15 Miles, M., "Tuning and Evaluation of Anti-Roll Tanks on CFAV *Quest*," National Research Council of Canada Report LTR-SH-122, Jan. 1972.
- 16 Miles, M., Private communication.
- 17 Frank, W. and Salvesen, N., "The Frank Close-Fit Ship Motion Computer Program," DTNSRDC Report 3289, June 1970.

Appendix 1

Added-mass and damping coefficients in stability axes

The coefficients given in reference [4] apply to translating earth axes. The translation to stability axes is

$$\dot{\eta}_2 \rightarrow \dot{\eta}_2 + U \eta_6 = \dot{\eta}_2 + \frac{U}{i\omega} \dot{\eta}_6 = \dot{\eta}_2 - \frac{U}{\omega^2} \ddot{\eta}_6$$

$$\eta_4 \rightarrow \eta_4$$

$$\eta_6 \rightarrow \eta_6$$

Consider now the terms on the left-hand side (LHS) of the sway, roll, and yaw equations in reference [1]. Ignore the end-effect terms and perform the above axis transformation.

Sway:

$$\begin{aligned} & \left[\int_L a_{22} d\xi \right] (\ddot{\eta}_2 + U\dot{\eta}_6) + \left[\int_L b_{22} d\xi \right] \left(\dot{\eta}_2 - \frac{U}{\omega^2} \ddot{\eta}_6 \right) \\ & + A_{24} \ddot{\eta}_4 + B_{24} \dot{\eta}_4 + \left[\int_L a_{22} \xi d\xi + \frac{U}{\omega^2} \int_L b_{22} d\xi \right] \ddot{\eta}_6 \\ & + \left[\int_L b_{22} \xi d\xi - U \int_L a_{22} d\xi \right] \dot{\eta}_6 \\ & = \left[\int_L a_{22} d\xi \right] \ddot{\eta}_2 + \left[\int_L b_{22} d\xi \right] \dot{\eta}_2 \\ & + A_{24} \ddot{\eta}_4 + B_{24} \dot{\eta}_4 + \left[\int_L a_{22} \xi d\xi \right] \ddot{\eta}_6 + \left[\int_L b_{22} d\xi \right] \dot{\eta}_6 \end{aligned}$$

Roll:

$$\begin{aligned} & \left[\int_L a_{24} d\xi \right] (\ddot{\eta}_2 + U\dot{\eta}_6) + \left[\int_L b_{24} d\xi \right] \left(\dot{\eta}_2 - \frac{U}{\omega^2} \ddot{\eta}_6 \right) \\ & + A_{44} \ddot{\eta}_4 + B_{44} \dot{\eta}_4 + \left[\int_L a_{24} \xi d\xi + \frac{U}{\omega^2} \int_L b_{24} d\xi \right] \ddot{\eta}_6 \\ & + \left[\int_L b_{24} \xi d\xi - U \int_L a_{24} d\xi \right] \dot{\eta}_6 \\ & = \left[\int_L a_{24} d\xi \right] \ddot{\eta}_2 + \left[\int_L b_{24} d\xi \right] \dot{\eta}_2 \\ & + A_{44} \ddot{\eta}_4 + B_{44} \dot{\eta}_4 + \left[\int_L a_{24} \xi d\xi \right] \ddot{\eta}_6 + \left[\int_L b_{24} \xi d\xi \right] \dot{\eta}_6 \end{aligned}$$

Yaw:

$$\begin{aligned} & \left[\int_L a_{22} \xi d\xi - \frac{U}{\omega^2} \int_L b_{22} d\xi \right] (\ddot{\eta}_2 + U\dot{\eta}_6) \\ & + \left[\int_L b_{22} \xi d\xi + U \int_L a_{22} d\xi \right] \\ & \times \left(\dot{\eta}_2 - \frac{U}{\omega^2} \ddot{\eta}_6 \right) + A_{64} \ddot{\eta}_4 + B_{64} \dot{\eta}_4 \\ & + \left[\int_L a_{22} \xi^2 d\xi + \frac{U^2}{\omega^2} \int_L a_{22} d\xi \right] \ddot{\eta}_6 \\ & + \left[\int_L b_{22} \xi^2 d\xi + \frac{U^2}{\omega^2} \int_L b_{22} d\xi \right] \dot{\eta}_6 \\ & = \left[\int_L a_{22} \xi d\xi - \frac{U}{\omega^2} \int_L b_{22} d\xi \right] \ddot{\eta}_2 \\ & + \left[\int_L b_{22} \xi d\xi + U \int_L a_{22} d\xi \right] \dot{\eta}_2 \\ & + A_{64} \ddot{\eta}_4 + B_{64} \dot{\eta}_4 + \left[\int_L a_{22} \xi^2 d\xi \right] \ddot{\eta}_6 + \left[\int_L b_{22} \xi^2 d\xi \right] \dot{\eta}_6 \end{aligned}$$

Appendix 2

Bilge keel roll damping

Equations for the calculation of the coefficients C_0 , C_a , C_k , C_n , \textcircled{B} , F , and α in equation (56) are given in this Appendix. The coefficient F depends upon r , $\hat{\eta}_4$, T , b_k and Γ , the angle between the waterline, CG, and bilge keel root (Fig. 19):

$$F = \frac{3.13r\hat{\eta}_4}{T\sqrt{gb_k}} \Gamma^{1.7} \quad \alpha = 0.6 - 2.03 \exp(-25\xi)$$

The index α is also a function of r , b_k and Γ :

$$\alpha = 0.6 - 2.03 \exp(-25\xi)$$

where

$$\xi = b_k / (r\Gamma^{0.75})$$

The coefficient \textcircled{B} depends upon the length of girth from bilge keel root to waterline s , beam B , height of CG above keel \overline{KG} , draft d , and rise of floor F_r :

$$\textcircled{B} = \cos\gamma + \frac{s}{2b_k r} [q + p_0 - (p_0 - p_1)f(\lambda)]$$

where γ is the angle made by the plane of the bilge keel with the straight line passing through the CG and the bilge keel root.

$$q = \left[\frac{B}{2} \tan \left(\frac{\pi}{4} - \frac{\epsilon}{2} \right) + F_r - \overline{KG} \right] \sin \left(\frac{\pi}{4} + \frac{\epsilon}{2} \right)$$

$$\epsilon = \tan^{-1} \left[\frac{2F_r}{B} \right]$$

$$p_0 = \overline{KG} - \frac{d}{3} - \frac{2}{3} F_r$$

$$p_1 = 0.88 \left\{ \overline{KG} - d - 0.54 \right.$$

$$\left. \times \left[\frac{B}{2} - (d - F_r) \tan \left(\frac{\pi}{4} + \frac{\epsilon}{2} \right) \right] \right\}$$

$$f(\lambda) = \frac{1.34 \sin \frac{\pi\lambda}{3.6}}{1 + 0.162 \sin \left[\frac{\pi}{1.8} (\lambda - 0.9) \right]}$$

$$\lambda = \frac{R}{d - \frac{F_r}{B} (B - 2R)}$$

C_n is the normal pressure coefficient for a rectangular plate moving with a uniform velocity in the direction perpendicular to its plane:

$$C_n = \frac{1.98 \exp(-11b_k/l)}{1.17}, \quad b_k/l < 0.048$$

$$C_n = 1.17, \quad b_k/l \geq 0.048$$

The coefficient C_k depends upon ship form and in particular upon R , the bilge radius:

$$C_k = 1 + 3.5e^{-9k}$$

$$k = \frac{R(1 + F_r/B)^2}{(B \overline{KG}/2)^{1/2}}$$

C_a is a function of the rolling Reynolds number R_N , given by

$$R_N = \frac{8b_k r \hat{\eta}_4}{T\nu}$$

where ν is kinematic viscosity.

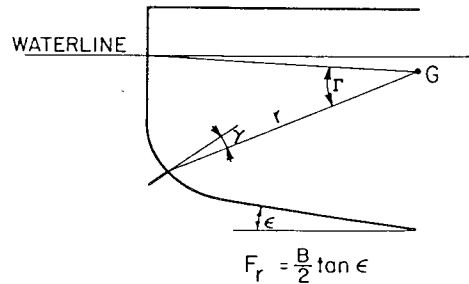


Fig. 19 Bilge keel parameters

$$C_a = \begin{cases} 1, R_N \geq 10^3 \\ 1.95 - 0.25 \log R_N + 0.2 \sin \left[\frac{\pi}{0.54} (\log R_N - 2.19) \right], \\ R_N < 10^3 \end{cases}$$

Finally, the coefficient C_0 depends upon Γ and also serves to scale the overall equation

$$C_0 = 14.1 + 37.3\Gamma^3$$

Appendix 3

Eddy-making roll damping

Empirical equations based on Tanaka's results [6] are presented here for evaluation of C , the eddy-making drag coefficient.

Consider first V- or U-shaped sections, Fig. 20(a), as are encountered in the foremost part of a ship. Tanaka has obtained the following empirical equation

$$C = T_1(B/\overline{KG})T_2 \left(\alpha, \frac{R_e}{d} \right) \exp \left(-u \frac{R_e}{d} \right) \quad (112)$$

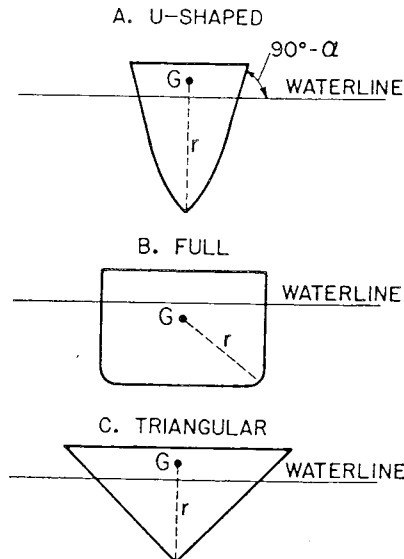


Fig. 20 Hull sections for eddy-making calculations

Table 1 T_1 versus B/\overline{KG}

B/\overline{KG}	T_1
0.0	0.50
0.25	0.61
0.5	0.62
1.0	0.61
1.5	0.53
2.0	0.40
2.5	0.35
3.0	0.32
3.5	0.29
4.0	0.26

Table 2 T_2 versus α and R_e/d

α (deg)	$R_e/d = 0$	0.0571	0.1142	0.1713
0	1.00	1.00	1.00	1.00
5	0.86	0.75	0.74	0.70
10	0.77	0.67	0.72	0.72
20	0.68	0.75	0.89	1.20
30	0.65	0.92	1.34	1.94

where α is the angle of inclination of the ship side at the waterline [Figure 20(a)], R_e is the effective radius at the keel, and u is a function of $\hat{\eta}_4$. T_1 and T_2 are given in Tables 1 and 2, respectively. Empirical equations for R_e and u , obtained by fitting least-squares quadratics to Tanaka's data, are

$$u = 14.1 - 46.7\hat{\eta}_4 + 61.7\hat{\eta}_4^2$$

$$R_e = \frac{B}{2} \left[4.12 - 2.69 \frac{\overline{KG}}{B} + 0.823 \left(\frac{\overline{KG}}{B} \right)^2 \right], \frac{\overline{KG}}{B} < 2.1$$

$$0, \frac{\overline{KG}}{B} \geq 2.1 \quad (113)$$

Consider now very full, almost rectangular, sections, as shown in Fig. 20(b). Equations (112) and (113) are used with r the distance from the CG to the bilge, R_e the bilge radius, and $T_2 = 1$.

Finally, consider triangular sections, Fig. 20(c), as are found farthest aft in cruiser-stern ships. For these sections, C is a function of B/\overline{KG} alone. The following quadratic has been fitted to Tanaka's data

$$C = 0.438 - 0.449(B/\overline{KG}) + 0.236(B/\overline{KG})^2$$

B_E is calculated by a strip method, with each section either placed in one of the above three categories or neglected. An example of a section whose eddy-making is negligible is a destroyer midsection with extremely rounded bilges and no skeg.

Appendix 4

Hull friction roll damping

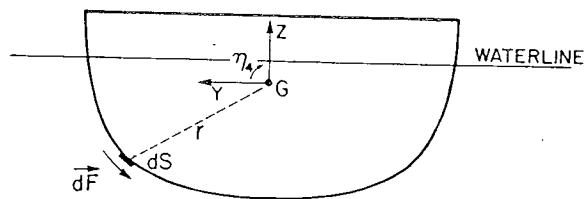


Fig. 21 Hull section showing dS and $d\vec{F}$

Consider an element of hull surface dS , Fig. 21. The skin friction drag force $d\vec{F}$ acting on dS as a result of the rolling velocity $\hat{\eta}_4$ is given by

$$d\vec{F} = \frac{1}{2} \rho r (y n_2 + z n_3) \hat{\eta}_4 |\hat{\eta}_4| C_{DF} dS (n_3 \vec{j} - n_2 \vec{k})$$

where C_{DF} is the skin friction drag coefficient, \vec{j} and \vec{k} are unit vectors along the y and z axes, and

$$r = \sqrt{y^2 + z^2}$$

is the distance from dS to the CG.

$d\vec{F}$ exerts a torque about the rolling axis given by

$$dT = -\frac{1}{2} \rho r (y n_2 + z n_3)^2 \hat{\eta}_4 |\hat{\eta}_4| C_{DF} dS$$

The energy dissipated by dT during one roll cycle is

$$dE = \frac{4}{3} \rho r (y n_2 + z n_3)^2 \omega^2 \hat{\eta}_4^3 C_{DF} dS$$

Hence, upon integrating dS over the hull by a strip method, equation (63) is obtained.

Appendix 5

Long-wave approximations for the forcing functions

Approximations valid for waves long relative to ship beam will now be derived for the forcing functions. Consider first the sectional wave incident force derived from strip theory, equation (26), and expand the complex exponential in the integral to give

$$I = \int_{C_x} n_j \exp(k_w z') (\cos p + i \sin p) dl$$

where, for convenience

$$p = k_w y \sin \beta_s$$

From symmetry considerations, the $n_j \cos p$ term integrates to zero for $j = 2, 4$, since n_j (port) = $-n_j$ (starboard). Hence

$$I = i \int_{C_x} n_j \exp(k_w z') \sin p dl$$

We now replace the exponential term in the integral by

$$e_H = \exp(-k_w c_a d) \quad (114)$$

where c_a and d are sectional area coefficient and draft, respectively. This is the approximation commonly employed in conjunction with the use of Lewis forms to compute sectional added mass and damping [17]. Note that this approximation is particularly valid for wavelengths long relative to beam, wherein the following also holds:

$$\sin p = p \quad (115)$$

The integral then becomes

$$I = i e_H k_w \sin \beta_s \int_{C_x} n_j y dl$$

Now, for $j = 2$, since $n_2 = dz/dl$,

$$I = i e_H k_w \sin \beta_s \int_{C_x} y dz = \overline{i e_H k_w} \sin \beta_s A_x \quad (116)$$

where A_x is sectional area.

For $j = 4$, from equation (28)

$$I = i e_H k_w \sin \beta_s \int_{C_x} (y n_3 - z n_2) y dl = -i e_H k_w \sin \beta_s M_x \quad (117)$$

where M_x is the sectional contribution to the roll-restoring moment (see Appendix 6).

Combining equations (26), (116), and (117) yields the approximations for the sectional incident forces given by equations (77) and (78).

Consider next the sectional diffraction force, equation (27), and expand the complex exponential in the integral.

$$\begin{aligned} I &= \int_{C_x} \phi_j \exp(k_w z') (i n_3 - n_2 \sin \beta_s) (\cos p + i \sin p) dl \\ &= \int_{C_x} \phi_j \exp(k_w z') \{ i (n_3 \cos p - n_2 \sin \beta_s \sin p) \\ &\quad - n_3 \sin p - n_2 \sin \beta_s \cos p \} dl \end{aligned}$$

From symmetry considerations, the term in brackets multiplying i integrates to zero for $j = 2, 4$, since

$$\phi_j \text{ (port)} = -\phi_j \text{ (starboard)} \quad \text{for } j = 2, 4$$

$$n_2 \text{ (port)} = -n_2 \text{ (starboard)}$$

$$\sin p \text{ (port)} = -\sin p \text{ (starboard)}$$

Hence

$$I = - \int_{C_x} \phi_j \exp(k_w z') (n_3 \sin p + n_2 \sin \beta_s \cos p) dl$$

We now apply the approximations (114) and (115), as well as $\cos p = 1$, whence

$$I = -e_H \sin \beta_s \int_{C_x} \phi_j (n_2 + n_3 k_w y) dl$$

Now $y n_3 = n_4 + z n_2$, whence

$$I = -e_H \sin \beta_s \int_{C_x} \phi_j [n_2 (1 + k_w z) + k_w n_4] dl$$

By definition [1]

$$\int_{C_x} \phi_j n_k dl = \frac{i}{\rho \omega} (\omega^2 a_{kj} - i \omega b_{kj})$$

whence equation (70) is obtained.

γ_j is a function of k_w , defined by

$$\gamma_j = 1 + k_w \int_{C_x} \phi_j n_2 z dl / \int_{C_x} \phi_j n_2 dl \quad (118)$$

Note that $\gamma_j \rightarrow 1$ as $\omega_w \rightarrow 0$. Furthermore, over the frequency range of interest, one would intuitively expect the following approximation to hold:

$$\gamma_j = 1 - k_w \bar{d} \quad (119)$$

where $h_{CC} \leq \bar{d} \leq h_{CC} + d$.

Consider now the foil exciting forces, beginning with sway. From equations (46) and (49), using the long-wave approximation for $\exp(i k_w y \sin \beta_s)$ and setting $G(k) = 1$ since the frequency is low

$$\begin{aligned} F_2^F &= -a \omega_w \sum e_F \exp(-i k_w x \cos \beta_s) \\ &\quad \left(\frac{1}{2} \rho U S C_{L\alpha} + i \omega a_p \right) \sin \Gamma \\ &\quad (\sin \Gamma \sin \beta_s + i \cos \Gamma) (1 + i k_w y \sin \beta_s) \\ &= -a \omega_w \sum e_F \exp(-i k_w x \cos \beta_s) \left(\frac{1}{2} \rho U S C_{L\alpha} + i \omega a_p \right) \sin \Gamma \\ &\quad [\sin \beta_s (\sin \Gamma - k_w y \cos \Gamma) + i (\cos \Gamma + k_w y \sin \Gamma \sin \beta_s^2)] \end{aligned}$$

where $e_F = \exp(-k_w h)$. Now from symmetry considerations the term multiplying i in the square brackets vanishes, leaving

$$\begin{aligned} F_2^F &= -a \omega_w \sin \beta_s \sum e_F \exp(-i k_w x \cos \beta_s) \\ &\quad \times \left(\frac{1}{2} \rho U S C_{L\alpha} + i \omega a_p \right) [\sin^2 \Gamma - k_w \sin \Gamma (\hat{y} - z \sin \Gamma)] \end{aligned}$$

since $y \cos \Gamma = \hat{y} - z \sin \Gamma$. From equations (32) to (35), then

$$\begin{aligned} F_2^F &= -a \omega_w \sin \beta_s \sum e_F \exp(-i k_w x \cos \beta_s) \\ &\quad \times [\gamma_F (b_{22}^F + i \omega a_{22}^F) + k_w (b_{24}^F + i \omega a_{24}^F)] \end{aligned}$$

where a_{jk}^F and b_{jk}^F are the contributions of individual foil elements to A_{jk}^F and B_{jk}^F , respectively.

$$\gamma_F = 1 + k_w z \sin^2 \Gamma \quad (120)$$

is the foil counterpart to equation (118).

Applying the same approximations to the other foil exciting forces, we obtain the general long-wave approximation, equation (80).

Appendix 6

Roll-restoring moment

Consider an element of hull area dA , located at (x, y, z) . When the ship rolls through a small angle η_4 , the hydrostatic force acting on dA increases by

$$df = -\rho g \eta_4 y dA$$

df acts normal to the hull, with y and z components:

$$df_y = -n_2 df$$

$$df_z = -n_3 df$$

The rolling moment exerted by df is

$$\begin{aligned} dK &= ydf_z - zdf_y = (-yn_3 + zn_2)df \\ &= -\rho g \eta_4 y (-yn_3 + zn_2) dA \\ &= -\rho g \eta_4 y (-yn_3 + zn_2) dx dl \end{aligned}$$

Integration over the hull gives the total roll-restoring moment

$$K = -\rho g \eta_4 \int_L M_x dx$$

where M_x is the sectional contribution to the roll-restoring moment:

$$M_x = \int_{C_x} (-yn_3 + zn_2) y dl$$

Discussion

Adrian R. Lloyd,³ Visitor

I would like to congratulate the author on what must be regarded as a fundamental advance in the theory of ship behavior in rough weather. It is easy to be wise with the benefit of hindsight and Mr. Schmitke's lucid explanation of his theory, but one wonders why such an eminently practical and understandable approach has not been developed before. Perhaps we have been waiting for someone of Mr. Schmitke's caliber to show us how to do it.

The close working links which have been forged between the Defence Research Establishment Atlantic and the Admiralty Marine Technology Establishment Haslar recently enabled us to obtain a copy of a computer program based on the theory described in this paper. This puts me in the unusual position of being able to comment on the theory with the benefit of practical experience of its use.

The paper presents various impressive comparisons of theoretically and experimentally determined roll decay coefficients. However, none of these is for a ship with multiple stabilizer fins. In this case serious hydrodynamic interference effects occur which generally reduce the lift generated by the after fins. These effects were covered in detail in two recent RINA publications,^{4,5} although the treatment given there is appropriate to the case where the fins are oscillating to stabilize the ship in roll and the resulting roll motion is small.

Figure 22 shows how the trailing vortex flow field differs when the fins are fixed and the ship is rolling. The treatment given (footnote 4) is still appropriate if fin incidence β is replaced by pR/U and the vortex displacement $\zeta = \chi\gamma$ is replaced by $\zeta = \chi[(pR/U) - \gamma]$ (using the notation of footnote 4).

The interference will reduce the magnitude of the terms $B_{22}^F, B_{24}^F, B_{26}^F, B_{44}^F, B_{46}^F, B_{62}^F, B_{64}^F$, and B_{66}^F in ships fitted with multiple stabilizer fins. A complicating factor is that this effect exhibits peculiar nonlinearities arising from the fact that the vortex interference is greatest when the induced incidence due to rolling is small.

Figure 23 shows a comparison between measured and predicted roll decay coefficients for a model destroyer having four pairs of stabilizer fins. The theory overestimates the experimental results by something like 20 percent except at zero speed, where the comparison is very good. An approximate calcu-

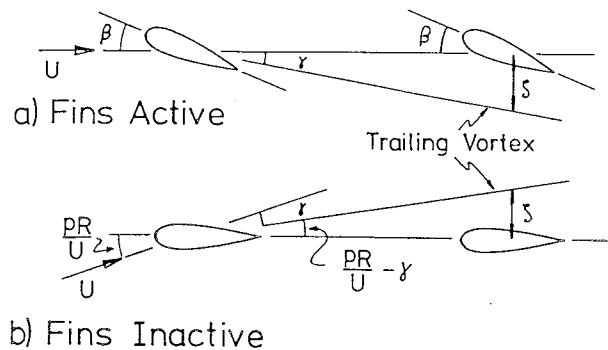


Fig. 22 Hydrodynamic interference between stabilizer fins

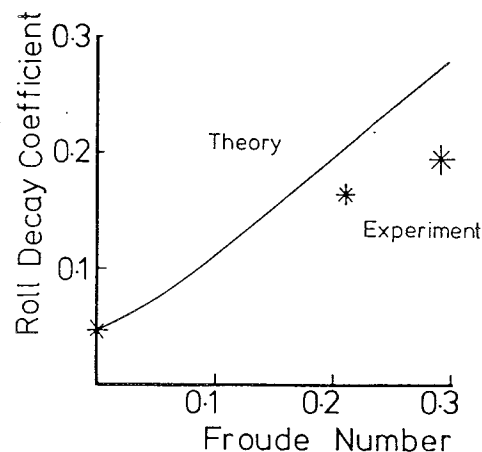


Fig. 23 Roll decay coefficients for a model destroyer with four pairs of stabilizer fins

lation along the lines just indicated suggests that in this particular case the contribution of the stabilizer fin lift to the roll damping is actually about one third of that predicted if interference is ignored. No doubt this explains the discrepancy between theory and experiment in this case.

The theory presented in the paper admits no contributions from the propeller shaft(s) and propeller(s). Would the author care to comment on this?

Finally, I believe the definition of \hat{y} in the Nomenclature to be incorrect. This should read "foil roll lever arm."

³ Admiralty Marine Technology Establishment, Haslar, Gosport, Hants, U.K.

⁴ Lloyd, A.R.J.M., "Roll Stabiliser Fins: A Design Procedure," *Transactions*, Royal Institution of Naval Architects, Vol. 117, 1975.

⁵ Lloyd, A.R.J.M., "Roll Stabiliser Fins: Interference at Non-Zero Frequencies," *Transactions*, Royal Institution of Naval Architects, Vol. 119, 1977.

Allen H. Magnuson, Member

This paper brings the art of ship motion prediction full circle. Korvin-Kroukovsky's empirical strip theory opened the modern era in ship motion prediction. The strip theory was subsequently put on a sound theoretical basis by Ogilvie, Tuck, Haskind and Newman. However, roll predictions were still unsatisfactory. Now Schmitke has returned to empiricism to supplement the hydrodynamic strip theory with a refined roll damping prediction technique that provides good agreement with experiment. The author's contribution represents an important milestone in ship motion prediction.

The author's achievement clearly illustrates the benefits of cross-disciplinary education and experience for engineers and researchers. Before attacking displacement ship seakeeping, the author worked on the dynamics of hydrofoil craft. This experience with lifting-surface theory and the aircraft type of dynamic analysis led him naturally to include the effects of lifting-surface-type appendages.

While I have not had time to go over the paper in detail, I do have a few comments and questions regarding some technical points. The first comment concerns the use of body-fixed or stability axes instead of earth-fixed axes. This is the first major seakeeping paper to put body axes to good use. Body axes are almost invariably used in ship and aircraft stability and control studies, as well as for hydrofoil craft dynamics. This axis system is the natural one to use for time-domain analysis of ship response to waves while maneuvering, and for analysis of additional nonlinear effects such as crossflow drag. This paper, then, represents a starting point for whole new areas of study.

There are several points on the correlation of the theory with full-scale trial data that are not clear. The first is, are the predictions of roll motion for oblique (nonbeam) seas based on the coupled roll-yaw-sway equations or on uncoupled roll? The decoupling of roll from yaw and sway was justified for only the beam sea case. I would expect from the beam sea analysis that roll could be uncoupled from yaw and sway in oblique seas provided the wavelength as projected on the longitudinal axis is much larger than the ship length. This is a more restrictive condition than for beam seas. In this case the ship would (to the first order) yaw and sway with the wave orbital velocity at the mean draft. What are the author's views on coupling in oblique seas?

Another question concerns the quasi-linearization used for quadratic roll damping. The quasi-linearization in the text is applicable only to regular sinusoidal waves. What was done for the random-wave response predictions?

The long-crested wave assumption used by the author produced good correlation with trial data. Whether the waves were in fact long-crested or not depends upon the amount of swell energy relative to the short-crested wind wave energy. This can usually be inferred from the wave spectra. Inclusion of the wave spectra would have been a valuable addition to the paper. Can the author provide any additional information on the wave conditions during the ship trials?

Geoffrey G. Cox, Member

[The views expressed herein are the opinions of the discussor and not necessarily those of the Department of Defense or the Department of the Navy.]

A few of us were already aware of the author's work to improve the accuracy of lateral motion predictions through his previous Defence Research Establishment Atlantic publications and his paper to the 18th American Towing Tank Conference. He is to be thanked for making his work generally available through this paper, and particularly commended for his identification of appendage dynamic lift effect as a major cause of

SR-161 CARGO SHIP

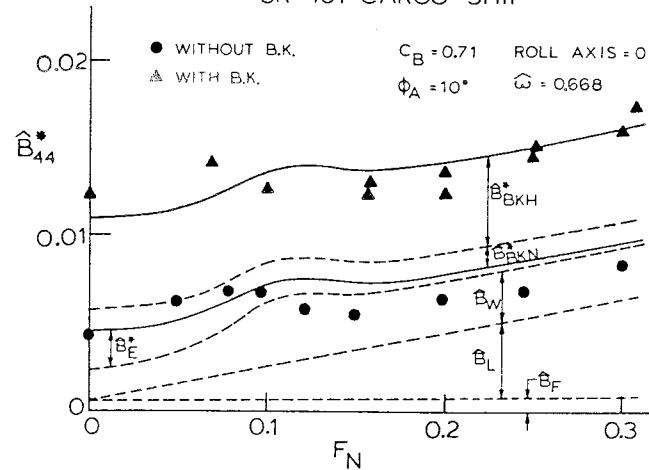


Fig. 24 Roll damping coefficient \hat{B}_{44}^* at forward speed (see footnote 7)

SR-161 CARGO SHIP

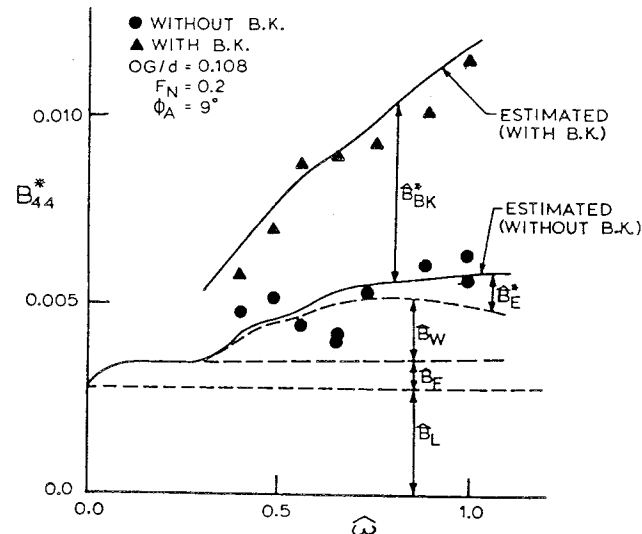


Fig. 25 Roll damping coefficient \hat{B}_{44}^* at $F_N = 0.2$ (see footnote 7)

roll damping dependence on ship speed.

The problem of upgrading the accuracy of ship roll motion predictions was an important topic for the Seakeeping Committee of the 15th International Towing Tank Conference.⁶ It reported on the author's work toward accurate prediction of roll damping, and also drew attention to a coordinated and extensive program of experimental and analytical work into the various components of roll damping carried out under the auspices of Research Panel SR161 for the Shipbuilding Association of Japan. Figures 24 and 25 taken from the Japanese work,⁷ and already shown to the 15th ITTC, give two samples of their comparisons between analytical predictions and model experimental data for the roll damping coefficient as a function

⁶ Seakeeping Committee Report, 15th International Towing Tank Conference, The Hague, The Netherlands, Sept. 1978; also, SR161, "Researches on Improvement of the Accuracy for Estimating the Seakeeping Qualities of Ships and Its Verification," Technical Memorandum of Japanese Shipbuilding Research Association.

⁷ Japanese Shipbuilding Research Association, No. 291, March 1978.

of Froude number and frequency, respectively. Here the predicted components of roll damping are identified by subscripts F for frictional, L for dynamic lift, E for hull eddymaking, W for wavemaking, BKN for bilge keel eddymaking, and BKH for the hull pressure change due to bilge keels.

With regard to this latest Japanese work to establish experimentally verified analytical formulations and empirical formulas for the important components of roll damping, it should be noted that analytical formulations using sectional Lewis form coefficients are used for computing the components for hull pressure change due to bilge keels⁸ and zero-speed hull eddymaking.⁹ Also, the following empirical corrections are used for forward speed effects

$$\text{Hull eddymaking}^{10} B_E = B_{EO} \left[1 + 625 \left(\frac{U}{L\omega} \right)^2 \right]^{-1}$$

$$\text{Hull friction}^{11} B_H = B_{HO} \left[1 + 4.1 \left(\frac{U}{L\omega} \right) \right]$$

Using the author's notation and subscript zero for zero speed, with Kato (author's reference [7]) used for B_{HO} .

I invite the author's comments on the following three points. First, can the use of a steady flow drag coefficient, that is, the Schoenherr skin friction drag coefficient of equation (65), be justified to describe an oscillating phenomenon in his equation (63) for the value of B_H at low to moderate forward speeds? Second, an important hull circulatory term B_{44}^C appears to be omitted? Such a dynamic lift term for the hull considered as a low-aspect-ratio wind and linearly dependent on forward speed is shown as B_L in Figs. 24 and 25 for the Japanese data. Third, why is the coordinate axes system described as fixed in the ship when the effect of ship roll on the coordinate system is ignored?

Yoji Himeno,¹² Visitor

It is my great pleasure to discuss this valuable paper. At first I would like to express my appreciation for using a couple of Japanese works in your prediction formula for ship rolling. I also agree with your opinion that the dynamic lift on appendages and the circulation effects on the ship hull are quite important problems.

We, the group of the University of Osaka Prefecture (Y. Ikeda, Y. Himeno, and N. Tanaka), have recently been occupied with research work on the prediction of ship rolling. However, we have some different opinions from yours concerning the components of roll damping, especially in the presence of ship speed:

1. The dynamic lift of the hull itself due to the roll motion has an important influence on the roll damping.
2. The wavemaking damping varies considerably with increasing Froude number and it has a hump at the point $\tau = 1/4$.
3. The nonlinear eddymaking damping almost vanishes in the high-speed range.
4. The nonlinear part of bilge keel damping decreases at high speed, while its linear part increases.

Therefore the reason why the viscous damping decreases in

⁸ Japanese Shipbuilding Research Association, No. 275, March 1977, pp. 6-8.

⁹ Ikeda, Y. et al, "On Eddy Making Component of Roll Damping Force on the Bare Hull," *Journal of Zosen Kiokai*, Society of Naval Architects of Japan, Vol. 142, Dec. 1977, pp. 54-69.

¹⁰ Ikeda, Y. et al, "Components of Roll Damping of Ship at Forward Speed," *Journal of the Society of Naval Architects of Japan*, Vol. 143, 1978.

¹¹ Tamiya, S. and Komura, T., "Topics on Ship Rolling Characteristics with Advance Speed," *Journal of Zosen Kiokai*, Society of Naval Architects of Japan, Vol. 132, Dec. 1972, pp. 159-168.

¹² Department of Naval Architecture, University of Osaka Prefecture, Osaka, Japan.

the high-speed range, and why the nonviscous component prevails as shown in Figs. 7 and 8 in the paper, seems to be partly because of these effects, as well as due to the dynamic lift on appendages as the author mentioned.

I would appreciate it if the author would comment on these points.

Donald McCallum, Member

[The views expressed herein are the opinions of the discussor and not necessarily those of the Department of Defense or the Department of the Navy.]

Mr. Schmitke and DREA, Halifax are both to be congratulated upon a fine paper, which, in my estimation, will go down as a landmark contribution in the area of prediction of ships motions in a seaway. The question which I have asked myself is, "Why didn't somebody do this before?" The basic theory has been with us for the past 20 years or so, and the effect that appendages have upon lateral ship motions is obvious when one takes the time to stop and think. In reading the paper, I am impressed by the clear and straightforward manner in which the theory is laid out, and can commend this paper to teaching institutions.

Several comments are germane. Mr. Schmitke states that "for ships of moderate to high metacentric height, rolling is greatest for seas on the beam." We of NAVSEC have found that maximum rolling usually occurs with sea direction between 60 and 75 deg from astern. This is borne out by Fig. 16, where the sea trials results suggest a maximum roll at about 65 deg.

Also I endorse Mr. Schmitke's statement regarding the importance of the roll decay coefficient n as the parameter which determines peak response in beam seas, but since r is highly dependent upon the rolling moment of inertia, I_4 , I would ask that Mr. Schmitke show us how I_4 is obtained. Kato has derived an empirical formula for prediction of I_4 . I am curious to know if Mr. Schmitke uses this in his method.

I am a little confused by Figs. 8 and 9, which are for a destroyer at its natural roll frequency. According to my scaling of Fig. 9, the percentage of viscous damping is 47 percent while on Fig. 8 this shows as being only about 25 percent. Could it be that Figs. 7 and 8 have been switched?

A comment about long-crested seas. Mr. Schmitke has validated his predictions by checking against full-scale tests performed on CFAV *Quest* and a Canadian destroyer, and long-crested seas were assumed to be present during these tests. The verification of the test results does indeed bear out the assumption of long-crested seas and I believe that this is a significant conclusion. This is also borne out by full-scale tests, also conducted by the Canadians, on a weathership, and reported in the 1969 *Transactions* of the Royal Institution of Naval Architects.¹³ It would be interesting for Mr. Schmitke to use these data as a further validation of the method outlined herein.

One final comment. We of the Naval Ship Engineering Center are impressed that Mr. Schmitke has used the FFG-7 model test results [12] as a validation of his technique. This ship was initially designed with no means of roll stabilization, except for bilge keels; however, as a result of an analysis using similar (but less sophisticated) roll prediction techniques, the U.S. Navy decided to install fin stabilizers, and a significant program is now underway to design, test and install a new generation of fins for this class of ship.¹⁴

¹³ Brunzell, P. A., Field, S. B., Martin, J. P., and Pangalila, F. V. A., "Correlation of Full Scale and Model Basin Stabilization Test Results for the Canadian Weatherships," *Trans.*, RINA, Vol. 111, 1969.

¹⁴ Nelson, L. and McCallum, D., "Fins of the Future—FFG-7," Association of Scientists and Engineers 15th Annual Symposium, 1978.

Thank you for a well-written and documented extension to the state-of-the-art in ship motions.

Nils Salvesen, Member

[The views expressed herein are the opinions of the discussor and not necessarily those of the Department of Defense or the Department of the Navy.]

It is generally recognized today that strip theory predicts the pitch and heave motions for most common hull forms with amazing accuracy. This paper shows that the roll motions can also be predicted by strip theory with good accuracy if the damping due to dynamic lift is included in addition to the damping due to viscous effects and wave generation. For the high-speed ships considered in the paper, it is found that the dynamic lift is the major part of the total roll damping in the important frequency range close to the natural frequency. Since dynamic lift is linear with respect to the motion amplitudes, this implies that linear models and linear superposition may be used and hence that the roll motions for high-speed ships in irregular waves may be computed with good accuracy using the standard linear procedure presently in use for predicting pitch and heave motions in irregular waves.

The method presented here predicts not only the roll motions but also the sway and yaw motions. However, I would like to stress that even though the roll motions are accurately predicted, this does not necessarily mean that the method is useful for predicting the sway and yaw motions. First of all, as pointed out by the author, due to lack of experimental data, an evaluation of the accuracy of the sway and yaw motions cannot easily be performed. But more importantly, in linear strip theory it is assumed that the responses are harmonic with frequency equal to the wave-frequency of encounter, whereas a ship in a seaway will experience slowly varying sway and yaw drift motions in addition to the motions with frequency components equal to the frequency of encounter of the individual wave components. In most engineering applications, it is the slowly varying drift motions which are of the greatest importance for the sway and yaw motions, since these motions usually result in the largest displacement. For a ship in bow waves, for example, the steering system is not designed to correct for the small high-frequency sway and yaw motions; it is only used to control the larger slowly varying sway and yaw motions. Since the slowly varying drift motions are caused by nonlinear wave excitation, which is not included in strip theory, we still lack adequate tools for solving the sway and yaw motion problems usually encountered in ship and platform design.

In summary, I find this a remarkable paper. It was only last year that Professor J. N. Newman stated very correctly in his review article on "The Theory of Ship Motions" that "no satisfactory method exists for predicting the rolling motion of ships with engineering accuracy." The results presented in this present paper seem to show that we now finally have the missing tool for predicting the roll motions. I would like to congratulate the author for this major and important contribution to the field of ship motions.

Haruzo Eda, Member

• *Yaw-roll coupled instability*—When a ship is proceeding at a high speed in a seaway, serious rolling motions are frequently observed in actual ship operations and in model testing in waves. Anomalous behavior or rolling and steering was clearly evident, for example, in full-scale tests of a high-speed container ship during transatlantic operations.

Certain high-speed ships have the following hull form characteristics which have major impacts on ship performance, in particular, on maneuvering and rolling behavior:

1. High speeds with large l/B ratio and relatively small GM .

2. Fore-and-aft asymmetry.

3. Relatively large rudder.

These particular hull form characteristics introduce the possibilities of fairly significant yaw-sway-roll-rudder coupling effects during high-speed operations.

Recently, a high-speed ship was extensively tested in the rotating-arm facility of the Davidson Laboratory, with inclusion of roll motion effect. Test results clearly indicated fairly significant couplings between yaw-sway-roll-rudder motions. Accordingly, a mathematical model was formulated on the basis of these experimental results combined with analytical estimations.

• *Asymmetry in underwater hull configurations due to roll*—Figure 26 shows two curves which indicate the distance of the CG of the local sectional area from the longitudinal centerline at roll angle $\varphi = 0$ and 15 deg. The curves can be considered to be equivalent to camberline of the wing section.

When the roll angle is not zero, the camberline is not a straight line, as shown in these figures introducing hydrodynamic yaw moment and side force. This trend is pronounced by the fore-and-aft asymmetry of hull form, in particular, during high-speed operation. Figure 27 shows, for example, captive model test results of the yaw-roll coupling effect, indicating hydrodynamic yaw moment to port introduced by roll angle to starboard.

When roll extinction curves were obtained in simulation runs in equations of roll-yaw-sway coupled motions, important results were shown in rolling and yawing behavior. Roll-yaw coupled instability was clearly indicated in test runs.

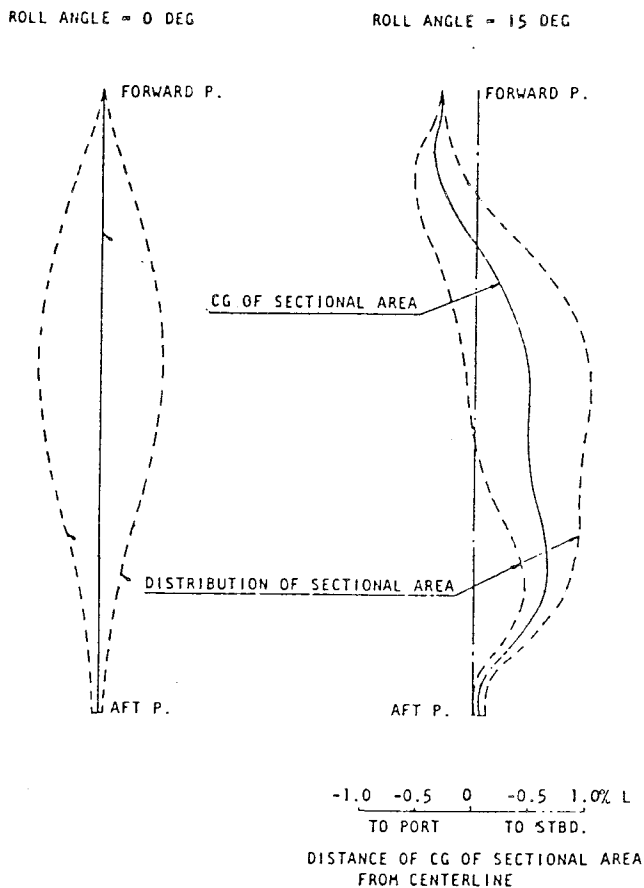


Fig. 26 Longitudinal asymmetry due to roll (high-speed container-ship)

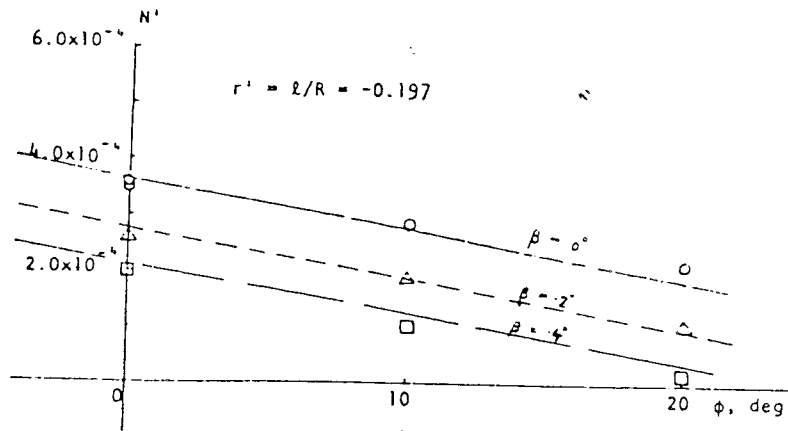


Fig. 27 Yaw moment coefficient due to roll angle

When the ship is rolled to the starboard, for example, due to beam wind from the port, an asymmetry is formed in the underwater portion of the hull as shown in Fig. 26. As a result, hydrodynamic yaw moment is generated to deviate the ship heading angle deviation. This starboard rudder angle produces the roll angle farther to the starboard. Under this condition, the possibility of instability exists in the ship systems.

Serious rolling problems frequently observed during high-speed operation in waves can partly be due to inherent yaw-roll instability (or marginal stability).

J. Mathisen,¹⁵ Visitor, and K. Lindemann,¹⁵ Visitor

With the presentation of this paper, the author has provided a valuable improvement to the techniques available for the calculation of lateral motions of ships. He stresses the importance of dynamic lift on the rolling behavior of fast warships.

We would like to ask a few questions, and present some comments related to the rolling of a different class of vessel, namely, barge-carrying offshore structures.

For a destroyer at 20 knots, Fig. 9 shows dynamic lift to account for over 50 percent of the damping at roll resonance and about 30 percent at higher frequencies. At zero speed, lift effects disappear and viscous damping dominates (Figs. 7 and 8). Low-speed barges have no dynamic lift. However, our calculations show that the importance of (nonviscous) wave damping is greatly increased for these shallow-draft vessels (see Fig. 28). This analysis includes viscous effects due to bilge keels, eddymaking, and hull friction, and (nonviscous) wave damping.

The roll response for barges is still believed to be overestimated, perhaps because the results of Kato's and Tanaka's work are being stretched outside the region where they may be legitimately applied. More work is surely necessary in this field.

A better appreciation of the relative importance of the various damping terms would be possible if the author could indicate the magnitude of the contribution from each term: bilge keels, eddymaking, skin friction, circulatory effects, dynamic lift, and wave damping.

When linearizing viscous damping, as in equations (58), (62), (63), and (69), it is necessary to estimate the roll amplitude ($\hat{\eta}_4$) prior to solving the equations of motion. This parameter can also be used to calculate an effective roll restoring coefficient instead of using the initial metacentric height. Using this modification in our ship theory program, we have obtained

significant variations in the roll resonance period and resulting roll angles. For some barges with predominantly nonviscous roll damping, this may lead to increased results for roll angle with increasing initially estimated roll amplitude ($\hat{\eta}_4$). This is the opposite of the usual tendency when viscous damping dominates and increased $\hat{\eta}_4$ gives increased damping only.

The appropriate value of $\hat{\eta}_4$ may be determined by a straightforward iterative technique in regular waves, but is difficult to define in irregular waves. Could the author explain how he chose suitable amplitudes ($\hat{\eta}_4$) for his comparison with sea trial data in Fig. 16?

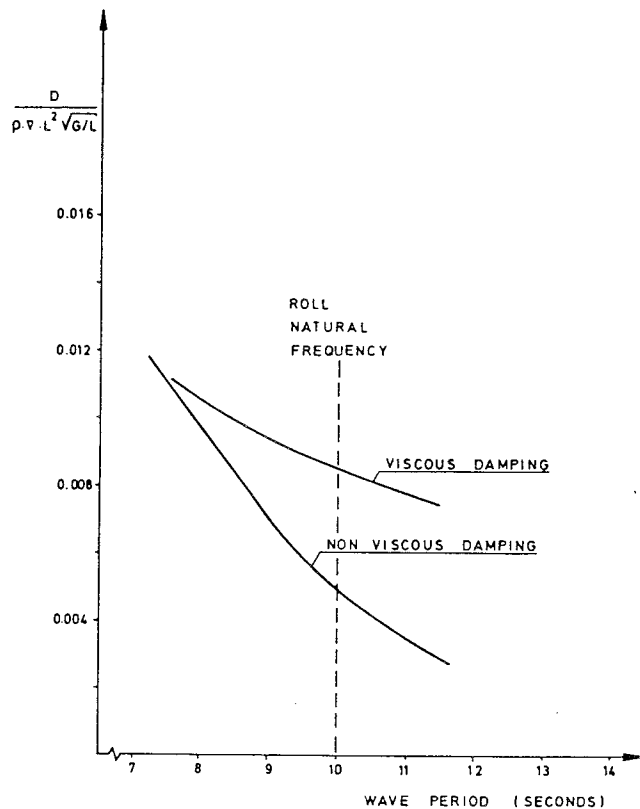


Fig. 28 Roll damping at zero speed for shallow-draft vessels

¹⁵ Det norske Veritas, Høvik, Norway.

Vladimir K. Ankudinov, Member

I would like to ask the author if there were special reasons to use long-wave approximations for the calculations of the wave exciting forces. Using the strip theory, excitation can be calculated easily without these restrictions.

One remark. Hydronautics, Inc. has a similar program for the prediction of roll motions, including the hull viscous effects and the lifting effects from the fin.

Author's Closure

Dr. Lloyd's comment on interference effects between multiple pairs of stabilizer fins underscores the need for careful attention to appendages, because of their dominant contribution to roll damping. This remark is very timely, since the computer program to which Dr. Lloyd refers is in the final stages of formal documentation, and his comment arrives in time for us to include interference effects on roll damping following the methods given in the two references he cites. Very little additional programming is required, since subroutines based on these methods are already in the program to account for downwash effects due to fin deflection.

Dr. Lloyd also raises the question of the contribution to roll damping of propellers and propeller shafts. First with regard to propeller shafts, at zero forward speed and zero speed of rotation, an expression similar to equation (69) could be used to estimate the shaft's contribution to viscous roll damping. Moreover, there now exists a literature on oscillating cylinders, from which more precise formulations could be derived, particularly with regard to frequency effects. However, once the shafts are rotating, the situation is much more complicated; the shaft is then a lifting body because of the Magnus effect, and both lift and drag are dependent on rotational velocity. Nonzero forward speed presents an additional important complication.

The general case is therefore quite complex. However, one can establish by rough calculations that for twin-screw ships with normally sized bilge keels, the contributions of propeller shafts to viscous roll damping at zero forward speed and zero rotation would be relatively small. Therefore, in view of the complexities outlined in the foregoing, it was decided not to include the effects of propeller shafts on roll damping. Subsequent correlation studies gave no reason to reverse this decision.

With regard to propellers, detailed consideration would clearly be impractical because of the complex geometry of propellers. However, it may be possible to formulate approximations based on such geometric parameters as diameter and blade/area ratio.

Before we leave this subject, I wish to emphasize that the decision not to include propellers and propeller shafts was taken on the basis of expediency, not rigor. Further work on this aspect of roll damping may be warranted.

In reply to Dr. Magnuson's query regarding the predictions of roll response given in Figs. 10-18, these have been made using the coupled sway-roll-yaw equations. With regard to coupling in oblique seas, this topic has been discussed in some detail by Cox and Lloyd [11]. My personal view on coupling is that use of an uncoupled equation to describe roll is probably a reasonable approximation for seas on or near the beam, when yawing is very small. At more oblique headings, one would intuitively expect coupling to become more important, because yaw is no longer negligible.

Dr. Magnuson also asks about the quasi-linear approximation to quadratic roll damping in random waves. Here, the procedure employed is to use the average roll amplitude, that is, 1.25 times the root-mean-square value.

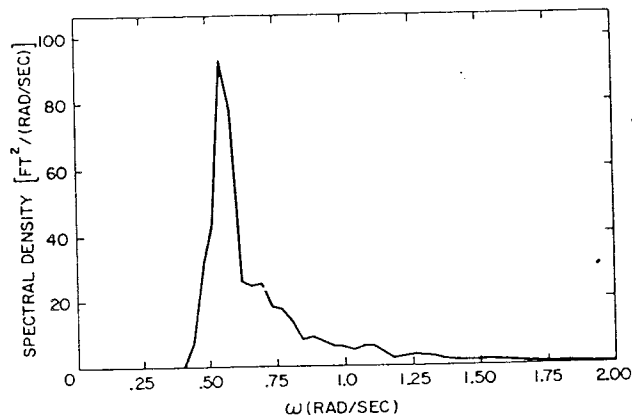


Fig. 29 Wave spectrum for *Quest* trial

Regarding the provision of additional information on the wave conditions encountered during the ship trials referred to in the paper, Fig. 29 shows the wave spectrum measured during the *Quest* trials. The spectrum is unimodal and rather sharply peaked. Significant wave height is 16.5 ft (5.02 m) and average period is 9.0 sec. The spectra measured during the destroyer trials were also unimodal, with significant wave height of roughly 17 ft (5.18 m).

I am indebted to Mr. Cox and Prof. Himeno for the information on recent and current Japanese work on roll damping, of which I was only slightly aware. I am especially grateful to Prof. Himeno for providing me with two of the references (footnotes 9 and 10) cited by Mr. Cox. It is most interesting that people working independently on opposite sides of the world should reach similar conclusions at approximately the same time. The resemblance of Fig. 25 to Fig. 9 is remarkable.

Both Mr. Cox and Prof. Himeno raise the issue of the contribution to roll damping of dynamic lift on the hull, which is ascribed considerable importance in the Japanese work cited by Mr. Cox. Although no expression for B_{44}^C is given in my paper, this does not mean that the effect of lift on the hull is ignored in estimating roll damping. The contribution of the skeg (sometimes referred to as deadwood [9]) is included, and for ships of the type investigated by Prof. Himeno and his colleagues, this can be shown to be the dominant source of lift-generated roll damping, as will now be demonstrated.

Ikeda et al (footnote 10) use the following expression for lift-generated roll damping, for cargo ships of normal hull form with $C_M > 0.97$:

$$B_L = \rho UT^4 (\pi + 0.62B/T - 0.0068L/T)(0.3 + \hat{h}_{CC})(0.5 + \hat{h}_{CC})$$

where $\hat{h}_{CC} = h_{CC}/T$. The corresponding term in the present paper, that is, roll damping due to skeg lift, is

$$B_{SK} = (\pi/2)\rho UT^4 \hat{h}_S^2 (1 + \hat{h}_{CC} - \hat{h}_S/3)^2$$

where $\hat{h}_S = h_S/T$ and h_S is skeg height at the trailing edge [9]. The very-low-aspect ratio approximation has been used for skeg lift curve slope, and the center of lift has been placed at the skeg centroid.

Typically, for single-screw merchant ships, \hat{h}_{CC} is near zero and \hat{h}_S near unity. For convenience, therefore, we will set $\hat{h}_{CC} = 0$ and $\hat{h}_S = 1$, whence

$$B_{SK}/B_L = 4.65/(\pi + 0.62B/T - 0.0068L/T)$$

For the ship models investigated by Ikeda et al (footnote 10), this equation gives the following results:

MODEL	L/T	B/T	B_{SK}/B_L
SR 98	16.8	3.06	0.95
SR 159	16.5	2.75	0.98
SR 108	18.4	2.67	1.00
Series 60, $C_B = 0.6$	18.8	2.47	1.02
Series 60, $C_B = 0.7$	17.5	2.50	1.02
Series 60, $C_B = 0.8$	16.2	2.50	1.01
SR 161	15.4	2.45	1.02

The above table clearly demonstrates that for single-screw merchant ships of normal hull form, the approach of the present paper gives roughly the same estimate of roll damping due to hull dynamic lift as the Japanese method. Including only the skeg in making this estimate is seen to be a valid approximation.

It is worthwhile discussing briefly the rationale underlying adoption of this approximation. Although the total sideforce acting on the hull at an angle of attack to the flow may be estimated with some pretense of accuracy, the distribution of this lift around the hull surface is largely a matter of conjecture, particularly for ships such as destroyers and frigates with extremely rounded bilges. The lift distribution due to rolling velocity involves an additional level of conjecture. Given the guesswork involved, the starting point chosen was to include skeg damping and ignore the rest of the hull. When this method proved to give satisfactory estimates of roll damping in practice, no further work was done on the problem. Admittedly, this is a procedure chosen on the basis of expediency, not rigor, and there is scope for further research.

Mr. Cox's point with reference to the use of the Schoenherr line to estimate C_{DF} is well taken. The empirical formulation of Tamiya and Komura (footnote 11) is probably a better approximation. As regards the query on ship-fixed axes, such an axis system is described in some detail in Section 3 of reference [9].

I am grateful to Prof. Himeno for informing us of the experimental results obtained at the University of Osaka on forward speed effects on wavemaking, eddy-making and bilge keel roll damping. When these results have been sufficiently generalized, they should be incorporated into ship motion computer programs. In the present paper, only bilge keel damping is dependent on forward speed, through equation (59), a linear term which increases with forward speed in accordance with Prof. Himeno's observation. As regards nonlinear damping, one would intuitively expect this to diminish with increasing speed, as lifting effects become more important.

Before we leave the subject of roll damping, I would like to make one final point. Good estimates of roll damping may be obtained in practice by thorough application of fundamental and well-established hydrodynamic principles, primarily to the

appendages and secondarily to the hull. No further fancy theoretical developments are required.

With regard to Mr. McCallum's comment on the direction of maximum rolling, the statement he refers to should read "on or near the beam." This would then include sea directions from roughly 70 to 110°. Clearly, the direction of maximum rolling depends on roll natural frequency, wave spectral content and ship speed, so making general statements is a risky business.

With regard to rolling moment of inertia, this has been estimated from the roll natural frequency. When the latter is unknown, it is recommended to use a value of total roll radius of gyration (structural plus hydrodynamic) between 35 and 40 percent of beam.

Mr. McCallum's observation regarding Figs. 7 and 8 is correct. This is rectified in the final text for TRANSACTIONS. As regards use of the Canadian weathership data for further correlation studies, this would be an interesting and useful project, but at present no effort is available at DREA for this purpose.

Dr. Salvesen's comment on sway and yaw prediction is very appropriate. Strip theory is known to have two major deficiencies with regard to sway and yaw. One is the phenomenon cited by Dr. Salvesen, due to nonlinear wave excitation. The other is unrealistically high prediction of sway and yaw displacement near zero wave encounter frequency. However, if velocities and accelerations are of interest rather than accelerations, strip theory may be adequate.

Dr. Eda introduces an interesting problem of practical importance for certain ship types. The implication is that for these ships $C_{24\eta_4}$ and $C_{64\eta_4}$ terms, especially the latter, should be added to the equations of motion, as well as rudder terms and a rudder system equation. It is worth noting that the latter are included in the DREA computer program referred to earlier.

I wish to thank Messrs. Mathisen and Lindemann for contributing several points of information on roll response of barges. Although barges are outside my range of experience, I certainly concur that knowledge is deficient regarding barge roll damping. Work on this subject should address wavemaking damping as well as viscous effects.

Finally, Mr. Ankudinov asks why the long-wave approximations to the forcing functions were introduced. The only reason for doing this was to facilitate the analysis of lateral motions in beam seas of long wavelength and thereby demonstrate theoretically that for this situation roll may be described by an uncoupled equation. In performing numerical calculations, these approximations are not used.

In closing, I wish to thank all the discussers for their very kind and illuminating submissions.